



UNIVERSIDADE FEDERAL DE SANTA CATARINA
CENTRO TECNOLÓGICO
PROGRAMA DE PÓS-GRADUAÇÃO EM ENGENHARIA QUÍMICA

Gabriel André Tochetto

**Acid attack followed by calcination treatment as a strategy for the development
of porous geopolymers applied to the adsorption of azo dyes**

Florianópolis
2023

Gabriel André Tochetto

Acid attack followed by calcination treatment as a strategy for the development of porous geopolymers applied to the adsorption of azo dyes

Master thesis submitted to the Programa de Pós-Graduação em Engenharia Química at the Universidade Federal de Santa Catarina as a partial requirement for obtaining the title of Master in Chemical Engineering.

Advisor: Ana Paula Serafini Immich Boemo, Dr.
Co-advisors: Dachamir Hotza, Dr.
Débora de Oliveira, Dr.

Florianópolis

2023

Tochetto, Gabriel André

Acid attack followed by calcination treatment as a strategy for the development of porous geopolymers applied to the adsorption of azo dyes / Gabriel André Tochetto ; orientador, Ana Paula Serafini Immich Boemo, coorientador, Dachamir Hotza, coorientador, Débora de Oliveira, 2023.

90 p.

Dissertação (mestrado) - Universidade Federal de Santa Catarina, Centro Tecnológico, Programa de Pós-Graduação em Engenharia Química, Florianópolis, 2023.

Inclui referências.

1. Engenharia Química. 2. Geopolímeros. 3. Adsorção. 4. Corantes. I. Boemo, Ana Paula Serafini Immich. II. Hotza, Dachamir. III. de Oliveira, Débora IV. Universidade Federal de Santa Catarina. Programa de Pós-Graduação em Engenharia Química. V. Título.

Gabriel André Tochetto

Acid attack followed by calcination treatment as a strategy for the development of porous geopolymers applied to the adsorption of azo dyes

The present work at the Master's level was evaluated and approved, on February 24, 2023, by the examining board composed of the following members:

Prof. Ana Paula Serafini Immich Boemo, Dr.
Universidade Federal de Santa Catarina
Advisor

Prof. Dachamir Hotza, Dr.
Universidade Federal de Santa Catarina
Co-Advisor

Prof. Débora de Oliveira, Dr.
Universidade Federal de Santa Catarina
Co-Advisor

Prof. Rui Miguel Novais, Dr.
Universidade de Aveiro
External Examiner

Prof. Agenor De Noni Júnior, Dr.
Universidade Federal de Santa Catarina
Internal Examiner

We certify that this is the original and final version of the final work that was considered suitable for obtaining the Master's Degree in Chemical Engineering.

Débora de Oliveira
Program Coordinator

Prof. Ana Paula Serafini Immich Boemo, Dr.
Advisor

Florianópolis, 2023

ACKNOWLEDGEMENTS

To my family! My mom Kika, my dad Alessio and my brothers Alexandre e Alex, thank you! You always believed in me, allowing me to fulfill dreams. When I needed you, you were always present. I said goodbye to Viadutos to now be in the place I always dreamed of, as you know Floripa became my home, but I never forgot my roots and teachings

To my friends! Some I met as a child, others during graduation, others still in the master's degree. But all of you, in one way or another, helped and supported me. Naming some people might be unfair, however, I especially need to thank Carol, Douglas and Vanessa. In moments of sadness and anguish, I could always count on your words of encouragement and affection. In moments of great joy, you were celebrating together. On the other days, you stayed with me. You made the walk lighter and more joyful. Our friendship is very special and I will continue to cultivate it.

To my advisors! Ana, you welcomed me as my first mentee at PósENQ and believed in my abilities as a researcher, thank you for the opportunity and for advising me throughout this period. Dachamir and Débora, thank you for agreeing to join this project, bringing new ideas and refining the work. Lisandro, thank you for your patience and teachings, working with geopolymers has become a pleasure. The results demonstrate the beautiful work developed by all of us.

I extend my thanks to the Graduate Program in Chemical Engineering (PósENQ) and the professors; the Mass Transfer (LabMASSA) and Ceramic Processing (PROCER) laboratories; the Universidade Federal de Santa Catarina (UFSC); to the Conselho Nacional de Desenvolvimento Científico e Tecnológico (CNPq). This research only happened thanks to your support.

Finally, thank you for reading this work! It was built with a lot of dedication in the hope that you can find the answers you are looking for and, above all, raise new questions.

*“Felicidade é a certeza de que a nossa
vida não está se passando inutilmente”*

– Érico Veríssimo.

ABSTRACT

Geopolymers (GP) are versatile materials initially developed to have high strength and density, being applied in the field of civil construction. However, GP intrinsically has micro and mesopores, so it was realized that these materials could be used in the environmental area, especially in the treatment of effluents. Soon, studies began to make the GPs more porous and with a larger specific area, allowing application in separation processes by adsorption and membranes. Thus, this dissertation aimed to study methods to modify the geopolymers, improving the essential properties and characteristics of a good adsorbent. As a strategy, the H₂SO₄ acid concentration (0-30%) and calcination temperature (200-600°C) were employed and evaluated through an experimental design (DCCR). Under optimized conditions for GP modification, it was observed that the contact with 15% H₂SO₄ followed by calcination at 200°C resulted in removal of about 98% of the direct red dye 28 (DR28) and adsorption capacity (q_e) of 40 mg g⁻¹. To understand the effect of changes caused by acid and temperature, geopolymers were characterized by surface functional groups (FTIR), mineralogical composition (DRX), morphology (SEM), chemical composition (EDS) and physical characteristics (BET/BJH). Kinetic studies demonstrate a good fit to the Elovich model and DR28 removals close to 100%. The adsorption isotherms suggest that the Sips model represents the data, noting $q_e = 109$ mg g⁻¹ at 50 °C. The modified GP had a 35% increase in q_e and color removal after regeneration, maintained for 3 cycles. The selectivity demonstrates a greater affinity for the direct dye, followed by acid, reactive, and disperse. From these results, it can be seen that the modifications were efficient to make GP a good adsorbent applied to the adsorption of azo dyes.

Keywords: Geopolymer; adsorbents; textile effluents; azo dyes.

RESUMO

Os geopolímeros (GP) são materiais versáteis, inicialmente desenvolvidos para ter alta resistência e densidade, sendo aplicados na área da construção civil. No entanto, o GP possui intrinsecamente micro e mesoporos, logo percebeu-se que esses materiais poderiam ser usados na área ambiental, especialmente no tratamento de efluentes. Logo, iniciaram-se estudos para tornar os GPs mais porosos e com maior área específica, possibilitando aplicação em processo de separação por adsorção e membranas. Assim, essa dissertação visou estudar métodos para modificar geopolímeros, melhorando as propriedades e características essenciais a um bom adsorvente. Como estratégia, a concentração de ácido H_2SO_4 (0-30%) e temperatura de calcinação (200-600 °C) foram empregados e avaliados por meio de um planejamento experimental (DCCR). Em condições otimizadas para modificação do GP observou-se que o contanto com 15% H_2SO_4 seguido de calcinação a 200°C resultaram na remoção de cerca de 98% do corante vermelho direto 28 (DR28) e capacidade de adsorção (q_e) de 40 mg g^{-1} . Para entender o efeito das modificações causadas pelo ácido e a temperatura, os geopolímeros foram caracterizados quanto aos grupos funcionais superficiais (FTIR), composição mineralógica (DRX), morfologia (MEV), composição química (EDS) e características físicas (BET/BJH). Os estudos cinéticos demonstram bom ajuste ao modelo de Elovich e remoções do DR28 próximas a 100%. As isotermas de adsorção sugerem que o modelo de Sips representa os dados, observando $q_e = 109 \text{ mg g}^{-1}$ em 50 °C. O GP modificado teve incremento de 35% no q_e e remoção de cor após a regeneração, se mantendo por 3 ciclos. A seletividade demonstra maior afinidade para o corante direto, seguido do ácido, reativo e disperso. A partir desses resultados, percebe-se que as modificações foram eficientes para tornar o GP um bom adsorvente aplicado a adsorção de azo corantes.

Palavras-chave: Geopolímeros; adsorventes; efluentes têxteis; azo corantes.

RESUMO EXPANDIDO

Ataque ácido seguido de tratamento de calcinação como estratégia para o desenvolvimento de geopolímero poroso aplicado à adsorção de corantes azo

Introdução

Os geopolímeros são polímeros inorgânicos com alto teor de silício e alumínio, ativados quimicamente e organizados em coordenação tetraédrica (Davidovits, 1991). Inicialmente desenvolvidos para aplicações na construção civil, demonstraram condições para uso em processos de separação por membranas e adsorção.

A imobilização de metais pesados e corantes tem sido o foco de pesquisas nos últimos anos e os resultados têm se mostrado promissores (Alouani et al., 2021; Tochetto et al., 2022b). No entanto, algumas estratégias podem ser utilizadas para incremento da porosidade, como o uso de aditivos.

Recentes estudos demonstram que o ataque ácido pode quebrar algumas ligações Si-O-Al, promovendo melhora na capacidade de adsorção (Chen et al., 2022), assim como a exposição do GP a altas temperaturas pode originar sítios de adsorção (Pan et al., 2023). No entanto, o efeito da combinação do ataque ácido seguido de calcinação não foi ainda explorado, mas a expectativa é a formação de um bom adsorvente.

O tratamento de águas residuárias de origem têxtil também representa um desafio, principalmente porque mesmo em baixas concentrações, o efluente ainda apresenta cor, causando impactos visuais e ambientais quando descartados em corpos d'água (Yagub et al., 2014). Os efluentes têxteis são compostos muitas vezes por uma mistura de corantes e, como há milhares de moléculas diferentes, as estações de tratamento podem não operar com eficácia.

Os azo compostos possuem o grupo cromóforo azo (-N=N-) e são a maior classe de corantes comerciais empregada na indústria têxtil, correspondendo a cerca de 70% de todos os corantes utilizados (Waring and Hallas, 1990). Esses azocorantes são de difícil degradação e sua remoção dos efluentes é imprescindível para evitar a poluição hídrica. Assim, estudos centrados na remoção dessa classe de corantes se torna necessária e justifica o presente trabalho.

Objetivo

O objetivo deste trabalho foi desenvolver um geopolímero poroso modificado com ataque ácido e calcinação, bem como avaliar o efeito das modificações nas características do adsorvente. Adicionalmente, pretendeu-se analisar a eficiência de remoção de azocorantes e obter os parâmetros cinéticos e termodinâmicos do processo adsorptivo.

Metodologia

Ensaio preliminares permitiram definir condições e formulações iniciais para a síntese do GP. A partir desses testes, decidiu-se utilizar 48 g de Na_2SiO_3 , 24 g de NaOH (8 M), 4 g de água destilada e 80 g de metacaulim (MK) para produção da pasta geopolimérica, que foi agitada a 250 rpm por 10 min. A mistura dos reagentes resultou numa razão molar $\text{SiO}_2/\text{Al}_2\text{O}_3 = 2.87$. A pasta foi colocada em moldes quadrados para cura a temperatura ambiente por 24 h. Posteriormente, o bloco foi moído e lavado até pH constante.

Para avaliar o efeito das modificações, um planejamento experimental (DCCR 2²) foi realizado, avaliando qual a concentração de H_2SO_4 e temperatura de calcinação ideal para promover os melhores resultados de adsorção do corante.

A fim de compreender o efeito das modificações, foram separadas amostras do GP sem nenhum tratamento (GP), com ataque ácido (GPA), com ataque ácido e calcinação (GPAT) e após o último ciclo de regeneração (GPAT-R) para caracterização física (BET/BJH), química (FTIR, EDS), mineralógica (DRX) e morfológica (MEV).

Foram definidas as condições ótimas para o desenvolvimento do GP: a melhor dosagem do adsorvente, a granulometria ideal e o pH da solução. Ensaio cinéticos de adsorção foram realizados em 4 concentrações de corantes (150, 220, 560 e 710 mg L^{-1}), onde 5 g L^{-1} de GPAT foi agitado a 200 rpm e 30 °C até o equilíbrio. As isotermas de adsorção foram avaliadas em 4 temperaturas (20, 30, 40 e 50 °C) com concentrações de corante variando de 100-1260 mg L^{-1} em sistema batelada (5 g L^{-1} de GPAT, 200 rpm, 120 min). O corante residual após adsorção foi analisado em espectrofotômetro.

Para descrever as cinéticas, foram utilizados os modelos de pseudo-primeira ordem, pseudo-segunda ordem e Elovich, enquanto os modelos de Langmuir, Freundlich e Sips foram usados para as isotermas.

A regeneração foi investigada após a saturação do GPAT, calcinando em 500 °C por 120 min. O ciclo foi repetido por cinco vezes.

A seletividade do GPAT foi avaliada em diferentes pHs (3-11) e usando os corantes vermelho direto 28, vermelho ácido 27, vermelho reativo 194 e vermelho disperso 343 (azocompostos com diferentes mecanismos de tingimento - direto, ácido, reativo e disperso - utilizados no tingimento de tecidos de diferente natureza química).

Resultados e discussão

Os resultados preliminares demonstraram que o H₂SO₄ e a calcinação aumentaram a remoção do corante, sendo confirmado experimentalmente. O planejamento experimental demonstrou que a concentração de ácido tem significativa influência, sendo possível determinar que 15% de H₂SO₄ e 200 °C são condições ideais para melhora na capacidade de adsorção. Na condição otimizada, observou-se remoção de 98,53% do DR28 e $q_e = 40,85 \text{ mg g}^{-1}$.

A caracterização revelou que os grupos funcionais se mantiveram semelhantes após as modificações, sendo observados principalmente picos referentes aos grupos O-H e Si-O-T (T = Si ou Al). A partir do DRX, verificou-se estrutura amorfa nos geopolímeros e na matéria-prima, e reflexões condizentes com caulinita em todas as amostras. No caso do GPAT, ainda se encontraram ilita e fosfato de alumínio. A morfologia mostrou que a superfície é irregular e as partículas possuem diferentes tamanhos e formatos. O EDS confirmou a presença de O, Na, Al e Si, elementos comuns ao GP, enquanto nas amostras que sofreram ataques ácido o S apareceu, originado do H₂SO₄. As propriedades texturais comprovaram que o H₂SO₄ e a calcinação foram estratégias eficazes para aumento da área específica em 4.2x (29 para 122 m² g⁻¹).

A granulometria de <425 µm, a dosagem de 5 g L⁻¹ de adsorvente e pH natural da solução foram as condições ótimas para prosseguir com os ensaios de adsorção. Foram observadas remoções próximas a 95% em 10 min de ensaio, enquanto $q_e \sim 90 \text{ mg g}^{-1}$ foi encontrado quando a cinética entrou em equilíbrio. O modelo de Elovich foi capaz de representar os dados cinéticos de forma adequada, indicando que a quimissorção tem forte influência no processo. As isotermas também se mostraram favoráveis, com bom ajuste do modelo de Sips e aumento do q_e com a temperatura ($qm = 107,5 \text{ mg g}^{-1}$).

A capacidade de adsorção aumentou de 28,6 para 43,8 mg g⁻¹ com a primeira regeneração. O *qe* se manteve por 3 ciclos, decaindo para 20.9 mg g⁻¹ no quarto ciclo, demonstrando a possibilidade de reciclo do adsorvente. O decréscimo no *qe* pode ser explicado pela redução da área superficial, enquanto o GPAT apresentou cerca de 122 m² g⁻¹ o GPAT-R, que foi caracterizado no quarto ciclo de sorção, teve área estimada em 33 m² g⁻¹.

Com relação à seletividade, o GPAT tem maior afinidade com o corante direto, seguido do ácido, reativo e disperso. Cabe ressaltar que, para o DR28, a faixa de trabalho se estende do pH 3 a 9 com alta eficiência.

Considerações finais

O ataque ácido seguido da calcinação demonstraram ser boas estratégias para o melhoramento de adsorventes geopoliméricos, promovendo a criação de poros e aumento da capacidade de adsorção. A possibilidade de usar o GPAT para outros corantes se mostra interessante, da mesma forma que a regeneração com incremento da remoção do corante torna o adsorvente competitivo e apto para ensaios em escala de colunas de adsorção e aplicação industrial.

Palavras-chave: Geopolímeros; adsorventes; efluentes têxteis; azo corantes.

LIST OF FIGURES

| | |
|---|----|
| Fig. 1 - Overview of publications relating geopolymers to adsorption from 1998 to 2022. | 25 |
| Fig. 2 - Thematic map of the most frequent keywords regarding geopolymers and adsorption from 2012 to 2022..... | 26 |
| Fig. 3 - Basic scheme for geopolymer synthesis (created in Chemix)..... | 27 |
| Fig. 4 - Geopolymer shapes: cylindrical (A), 3D-printed (B), granulated (C), spherical (D), and block (E) | 32 |
| Fig. 5 - XRD patterns of RHA (Rice Husk Ash), MK (Metakolin), GP (Geopolymer), and MGP (Mesoporous Geopolymer)..... | 34 |
| Fig. 6 - FTIR spectra of geopolymer adsorbent. | 37 |
| Fig. 7 - SEM micrographs of the (a) spheres' surface and (b) inner part after regeneration of the adsorbent and, (c) the EDS spectrum of the surface..... | 38 |
| Fig. 8 - Schematic illustration of MB adsorption mechanisms onto geopolymer..... | 43 |
| Fig. 9 - Characteristics of the azo dyes used in the adsorption tests of this work..... | 51 |
| Fig. 10 - Response surface as a function of (a) dye removal and (b) the adsorption capacity of the modified GP (Adsorption conditions: AD = 5 g L ⁻¹ , [DR28] = 200 mg L ⁻¹ , T = 30°C, A = 200 rpm, CT = 120 min, pH _i ≈ 7). | 60 |
| Fig. 11 - (A) DR28 removal kinetics and (B) adjustments of Elovich kinetic adsorption model to experimental data (Adsorption conditions: AD = 5 g L ⁻¹ , [DR28] = 150-710 mg L ⁻¹ , T = 30°C, A = 200 rpm, pH ≈ 7)..... | 64 |
| Fig. 12 - Isotherm adsorption curves for DR28 on GPAT fitted to the Sips model (Adsorption conditions: AD = 5 g L ⁻¹ , [DR28] = 100-1200 mg L ⁻¹ , T = 20-50°C, A = 200 rpm, CT = 120 min, pH ≈ 7)..... | 66 |
| Fig. 13 - Van't Hoff plot obtained from the thermodynamic study at different temperatures of DR28 adsorption in GPAT (Adsorption conditions: AD = 5 g L ⁻¹ , [DR28] = 100-1200 mg L ⁻¹ , T = 20-50°C, A = 200 rpm, CT = 120 min, pH ≈ 7)..... | 68 |

| | |
|--|----|
| Fig. 14 - Effect of GPAT regeneration on the adsorption capacity and removal efficiency of DR28 (Adsorption conditions: AD = 5 g L ⁻¹ , [DR28] = 400 mg L ⁻¹ , T = 30°C, A = 200 rpm, CT = 120 min, pH ≈ 7; Regeneration conditions: T = 500°C, CT = 120 min)..... | 70 |
| Fig. 15 - Evaluation of selectivity of GPAT for adsorption of azo dyes in a wide range of pH (Adsorption conditions: AD = 5 g L ⁻¹ , [DR28] = 200 mg L ⁻¹ , T = 30°C, A = 200 rpm, CT = 120 min). | 71 |
| Fig. 16 - FTIR spectra of material and geopolymer modified..... | 73 |
| Fig. 17 - XRD diffractograms of materials and modified geopolymer. | 74 |
| Fig. 18 – (a) Nitrogen adsorption/desorption isotherms and (b) pore size distribution of modified-GP. | 75 |
| Fig. 19 - SEM micrographs of (a) GP, (b) GPA, (c) GPAT, (d) GPAT-R and respective EDS analyses of the chemical elements identified. | 77 |

LIST OF TABLES

| | |
|--|----|
| Table 1 - Chemical composition of aluminosilicate sources for geopolymer synthesis. | 28 |
| Table 2 - Sources used for the synthesis of geopolymers and their physical characteristics. | 35 |
| Table 3 - Dyes removed by adsorption using geopolymers..... | 40 |
| Table 4 - Dye adsorption capacity (q_e) of geopolymer adsorbents | 43 |
| Table 5 – Factors and levels of the CCRD 22 experimental design matrix. | 52 |
| Table 6 - Analysis of different formulations of alkaline activators for geopolymerization (Adsorption conditions: $AD = 5 \text{ g L}^{-1}$, $[DR28] = 15 \text{ mg L}^{-1}$, $T = 30^\circ\text{C}$, $A = 200 \text{ rpm}$, $CT = 120 \text{ min}$, $pH_i \approx 7$). | 56 |
| Table 7 - Preliminary evaluation of acid attack (sulfuric acid and phosphoric acid) and calcination conditions for geopolymer modification (Adsorption conditions: $AD = 5 \text{ g L}^{-1}$, $[DR28] = 15 \text{ mg L}^{-1}$, $T = 30^\circ\text{C}$, $A = 200 \text{ rpm}$, $CT = 120 \text{ min}$, $pH_i \approx 7$). | 57 |
| Table 8 - Estimated effects, errors, and p -values of the adsorption capacity and dye removal on modified GP..... | 58 |
| Table 9 - Analysis of variance of the CCRD on the adsorption and removal capacity of the dye. | 58 |
| Table 10 - Experimental planning of GP production (real values) and responses regarding adsorption capacity and dye removal, and preliminary evaluation of pH effect (Adsorption conditions: $AD = 5 \text{ g L}^{-1}$, $[DR28] = 200 \text{ mg L}^{-1}$, $T = 30^\circ\text{C}$, $A = 200 \text{ rpm}$, $CT = 120 \text{ min}$, $pH_i \approx 7$). | 61 |
| Table 11 - Effect of particle size, adsorbent dosage, and pH value on DR28 adsorption (Adsorption conditions: $AD = 5 \text{ g L}^{-1}$, $[DR28] = 200 \text{ mg L}^{-1}$, $T = 30^\circ\text{C}$, $A = 200 \text{ rpm}$, $pH \approx 7$). | 63 |
| Table 12 - Kinetic parameters for DR28 adsorption onto GPAT (Adsorption conditions: $AD = 5 \text{ g L}^{-1}$, $[DR28] = 150\text{-}710 \text{ mg L}^{-1}$, $T = 30^\circ\text{C}$, $A = 200 \text{ rpm}$, $pH \approx 7$). | 65 |

| | |
|---|----|
| Table 13 - Isotherm parameters for DR28 adsorption onto GPAT (Adsorption conditions: AD = 5 g L ⁻¹ , [DR28] = 100-1200 mg L ⁻¹ , T = 20-50°C, A = 200 rpm, CT = 120 min, pH ≈ 7)..... | 67 |
| Table 14 - Thermodynamic parameters of DR28 adsorption on GPAT (Adsorption conditions: AD = 5 g L ⁻¹ , [DR28] = 100-1200 mg L ⁻¹ , T = 20-50°C, A = 200 rpm, CT = 120 min, pH ≈ 7)..... | 69 |
| Table 15 - Textural properties of modified GPs | 76 |

LIST OF ABBREVIATIONS

| | |
|---------|--|
| AC27 | Acid Red 27 |
| AD | Adsorbent Dosage |
| A | Agitation |
| BET | Brunauer, Emmett, Teller |
| BJH | Barrett-Joyner-Halenda |
| CCRD | Central Composite Rotatable Design |
| CT | Contact Time |
| DiR 343 | Disperse Red 343 |
| DR 28 | Direct Red 28 |
| EDS | Energy Dispersive Spectroscopy |
| FTIR | Fourier-Transform Infrared Spectroscopy |
| GP | Geopolymer |
| GPA | Geopolymer Modified with Acid |
| GPAT | Geopolymer Modified with Acid and Temperature |
| GPAT-A | Geopolymer Modified with Acid and Temperature after Adsorption |
| GPAT-R | Geopolymer Modified with Acid and Temperature after Regeneration |
| T | Temperature |
| MK | Metakaolin |
| RR 194 | Reactive Red 194 |
| SEM | Scanning Electron Microscopy |
| XRD | X-Ray Diffraction |
| [DR28] | Concentration of dye |

TABLE OF CONTENTS

| | |
|--|-----------|
| MASTER THESIS STRUCTURE | 20 |
| CHAPTER I..... | 21 |
| 1 MOTIVATION..... | 21 |
| 1.1 HYPOTHESIS..... | 21 |
| 1.2 OBJECTIVES..... | 22 |
| 1.2.1 General objectives | 22 |
| 1.2.2 Specific objectives..... | 22 |
| 1.3 CONCEPTUAL DIAGRAM..... | 22 |
| CHAPTER II..... | 23 |
| 2 LITERATURE REVIEW ON THE ADSORPTION OF DYES USING GEOPOLYMERS | 23 |
| 2.1 INTRODUCTION..... | 23 |
| 2.2 RESEARCH METHODOLOGY AND SCIENTOMETRIC ANALYSIS | 24 |
| 2.3 SYNTHESIS AND CHARACTERIZATION OF GEOPOLYMERS | 26 |
| 2.3.1 Geopolymer synthesis..... | 27 |
| 2.3.1.1 <i>Raw materials of geopolymers.....</i> | 28 |
| 2.3.1.2 <i>Porogenic agents</i> | 29 |
| 2.3.1.3 <i>Processing parameters</i> | 29 |
| 2.3.1.4 <i>Shaping of geopolymers</i> | 30 |
| 2.3.2 Geopolymer characterization..... | 32 |
| 2.3.2.1 <i>Microstructural analysis.....</i> | 32 |
| 2.3.2.2 <i>Physical analysis.....</i> | 34 |
| 2.3.2.3 <i>Chemical analysis</i> | 36 |
| 2.4 DYE ADSORPTION..... | 38 |
| 2.4.1 Dyes removed by adsorption..... | 38 |
| 2.4.2 Removal efficiency and adsorption mechanisms | 42 |
| 2.4.3 Desorption and regeneration | 45 |
| 2.5 CHALLENGES AND PROSPECTS | 46 |
| 2.6 CONCLUSIONS..... | 47 |
| CHAPTER III..... | 49 |
| 3 GEOPOLYMER DEVELOPMENT AND APPLICATION FOR DYE ADSORPTION | 49 |

| | | |
|--------------|---|-----------|
| 3.1 | INTRODUCTION..... | 49 |
| 3.2 | EXPERIMENTAL | 50 |
| 3.2.1 | Materials | 50 |
| 3.2.2 | Geopolymer preparation | 51 |
| 3.2.3 | Geopolymer modification | 51 |
| 3.2.4 | Evaluation of azo dye adsorption | 53 |
| 3.2.5 | Geopolymer regeneration | 54 |
| 3.2.6 | Selectivity of adsorbent..... | 55 |
| 3.2.7 | Raw materials and geopolymer characterization | 55 |
| 3.3 | RESULTS AND DISCUSSION..... | 55 |
| 3.3.1 | Preliminary tests to design the research | 55 |
| 3.3.2 | Influence GP modification | 57 |
| 3.3.3 | Evaluation of azo dye adsorption | 62 |
| 3.3.4 | Regeneration of GPAT | 69 |
| 3.3.5 | GPAT selectivity and effect of pH for azo dye adsorption | 70 |
| 3.3.6 | Effect of changes in GP characteristics..... | 72 |
| 3.4 | FINAL CONSIDERATIONS..... | 77 |
| | CHAPTER IV..... | 79 |
| 4 | CONCLUSIONS AND OUTLOOK..... | 79 |
| 4.1 | CONCLUSIONS..... | 79 |
| 4.2 | SUGGESTIONS FOR FUTURE WORK..... | 79 |
| | REFERENCES..... | 81 |

MASTER THESIS STRUCTURE

This dissertation was divided into four chapters.

Chapter I presents the motivation for the development of this research, as well as the hypotheses initially raised and the objectives to be achieved.

In Chapter II, a broad literature review was presented, addressing aspects of GP development and application in the adsorption of dyes.

Chapter III presents the experimental methodology for the synthesis of the modified geopolymer, as well as the results of the adsorption efficiency of azo dyes.

Chapter IV closes the research, answering the objectives through the conclusions and bringing future perspectives.

CHAPTER I

Chapter I briefly presents the motivations for this work, delimiting what the gaps are in the literature and presenting ways to respond to them. The hypotheses are formulated in the form of a question and the objectives of the work are then proposed.

1 MOTIVATION

The treatment of textile effluents still represents a challenge for industries. Conventional systems cannot completely remove the color, requiring advanced processes. Adsorption is an effective method for phase separation, transferring the dye from the liquid phase to the solid phase. This type of process allows the removal of compounds with high and low concentrations, being suitable as a tertiary treatment.

The selection of a good adsorbent is essential, but due to the high cost, alternatives to activated carbon are required. Thus, geopolymers appear as a possible substitute. Geopolymers are versatile and have simplified production but are dense and have low porosity.

The use of additives such as alumina powder, H₂O₂, and others can increase the specific area; however, recent studies suggest that acid attack and calcination may have more significant effects. So far, there are no studies that jointly correlate the effects of using these two strategies for modifying geopolymers.

1.1 HYPOTHESIS

- ✓ The acid attack causes the breaking of some Si and Al bonds.

Does this condition improve the properties of the adsorbent?

- ✓ Calcination is a common process in the production of activated carbons.

Is thermal treatment necessary to enhance the adsorption capacity?

Can the porous adsorbent with alkali activation and later modified with acid effectively adsorb cationic, anionic, and nonionic dyes (direct, acid reactive and dispersed)?

- ✓ The scale-up of the process requires of the reuse of adsorbents.

Thus, how many adsorption cycles can the produced geopolymers support, maintaining high efficiency?

1.2 OBJECTIVES

1.2.1 General objectives

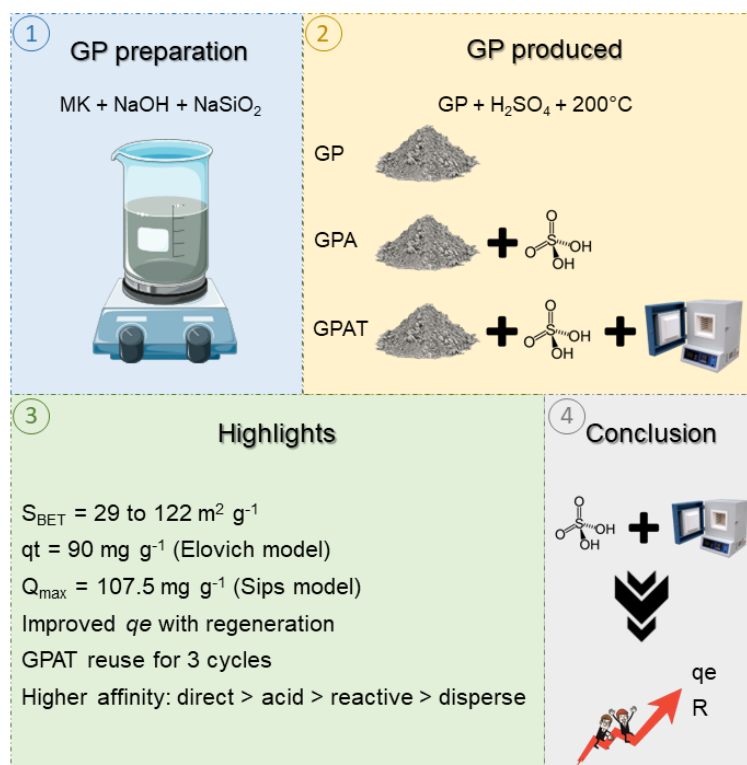
The general objective of this work was the development of an efficient porous geopolymer for the adsorption of azo dyes.

1.2.2 Specific objectives

The specific objectives are:

- Investigate the effects of acid attack and calcination on the geopolymer structure;
- Obtain the optimized conditions for modifying the adsorbent;
- Characterize the materials produced;
- Determine the best operational conditions for adsorption;
- Analyze the kinetic and thermodynamic parameters of dye adsorption;
- Investigate the effect of regeneration on the adsorbent;
- Evaluate the selectivity of the geopolymer for the sorption of different azo dyes.

1.3 CONCEPTUAL DIAGRAM



CHAPTER II

In this section, an analysis of the state of the art, as well as the gaps and challenges regarding the application of geopolymers in the adsorption of dyes, was conducted. The results found gave rise to the article *Porous geopolymers as dye adsorbents: review and perspectives*¹, published in the Journal of Cleaner Production. The objective of this chapter is to present geopolymer synthesis, pore formation strategies, and desirable characteristics of a good adsorbent. Still, it discusses the efficiency of the removal of dyes and the adsorptive capacity of geopolymers, the mechanisms of sorption, and the regeneration of the adsorbent.

2 LITERATURE REVIEW ON THE ADSORPTION OF DYES USING GEOPOLYMERS

2.1 INTRODUCTION

The combination of aluminosilicates with an activating solution is generally known as geopolymerization (Davidovits, 1991; Duxson et al., 2007). Geopolymers (GPs) are promising materials with a wide range of applications, e.g., building and construction, hydraulic works, refractory insulation, and removal of toxic substances from the environment (Duxson et al., 2007; Zhang et al., 2021). In the last decades, there has been an increase in new research on the use of porous geopolymers in purification, separation, and catalytic processes for water treatment (Alouani et al., 2021). Singh et al. (2018) suggested that GPs can be applied as adsorbents in wastewater treatment owing to their organizational structure. An ideal adsorbent material must have intrinsic properties such as high surface area, pore volume, and suitable pore distribution (Lee et al., 2016) properties which are usually found in GPs.

There is an always increasing search for new materials with high adsorption capacity, low cost, and environmental sustainability (Mo et al., 2018; Siyal et al., 2018). Wastewater treatment still poses a challenge to many industries that use dyes in their processes, e.g., textiles, plastics, and paper plants, because many dyes have high water solubility, which can be visible even in trace concentrations (Chen et al., 2019;

¹ Published in *Journal of Cleaner Production* 374 (2022) 133982
doi.org/10.1016/j.jclepro.2022.133982.

Crini, 2006). In addition, dye molecules may contain chromium, heavy metals, amines, aromatic rings, and other compounds, which are both carcinogenic and mutagenic. The effects on aquatic activity can be severely compromised when it is exposed to these dyes, especially reduced penetration of light into the water; also, humans can suffer organ dysfunction and changes in the body (Yagub et al., 2014).

This work presents aspects of the development of GPs and their desirable characteristics for consideration of appropriate adsorbents. Moreover, the efficiency of GPs in dye adsorption, the respective control mechanisms, and regeneration are also deeply discussed, pointing out some gaps and future perspectives for their use as promising adsorbents especially as far as dyes are concerned.

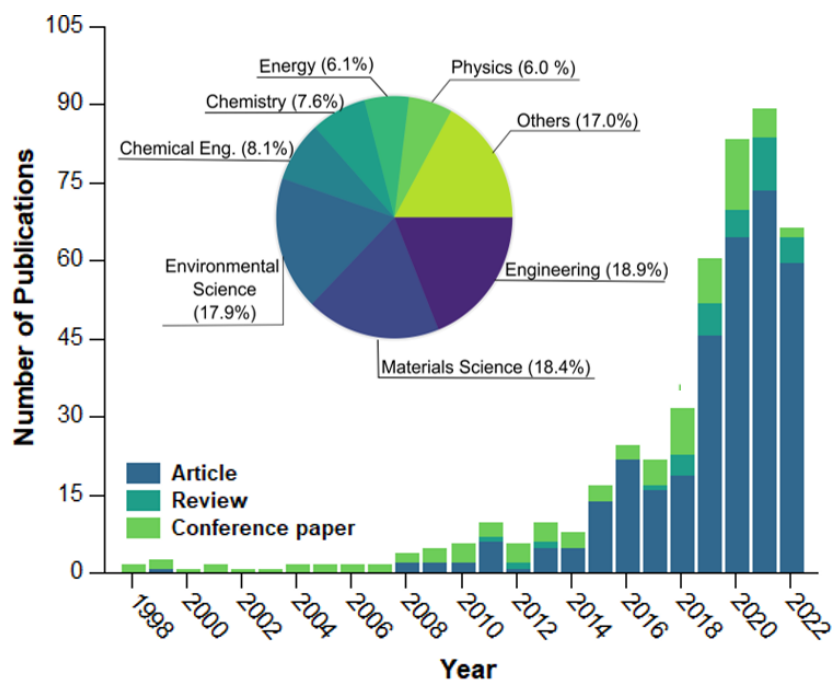
2.2 RESEARCH METHODOLOGY AND SCIENTOMETRIC ANALYSIS

This work used a systematic methodology for the bibliographic review. First, the articles were selected from Scopus (Elsevier's abstract and citation database), with software-supported bibliometric mapping (VOSviewer) (van Eck and Waltman, 2010).

The search for the terms “geopolymer*” and “adsorption” for the period from 1998 to 2022 resulted in 406 documents. The publications were classified into articles, proceeding papers, and reviews, as shown in Fig. 1. In addition, the article selection was based on title, highlights, and abstract; after that, the articles were read in full. Based on information collected from the articles, figures, and tables were prepared for compiling the literature data on the related subject.

In the last 10 years, more and more researchers were interested in evaluating GPs as adsorbent materials. The pie chart indicates that more than 55% of research is concentrated in the broad engineering field, including materials science, environmental science, and chemical engineering. The most frequent applications of porous GPs are in separation processes such as adsorption and membranes.

Fig. 1 - Overview of publications relating geopolymers to adsorption from 1998 to 2022.

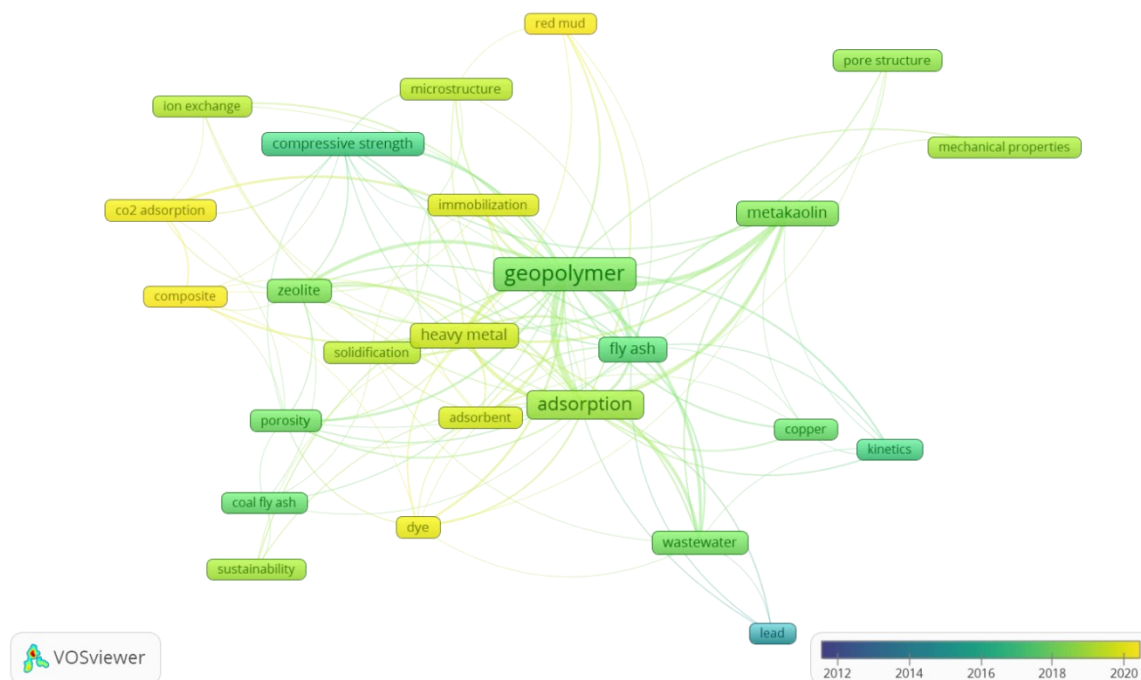


Source: the author

A thematic map (Fig. 2) was designed with the most frequent keywords mentioned by the authors. Most recent publications are given in yellow; the oldest ones, in blue. The adsorption of metal ions was one of the first interests in using GPs as adsorbents. The terms “lead”, “copper”, and “heavy metal” began to appear in 2015. Currently, GPs are employed to remove gases (e.g., CO₂) and dyes.

The bibliometric search resulted in the selection of 343 research articles that applied GPs in adsorption. However, as the objective was to particularly evaluate dye removal, those works related to metals, gases, and other pollutants were discarded. Thus, there were about 57 articles left, which describe the synthesis and properties of porous geopolymers applied as dye adsorbents. They will be further discussed in this work.

Fig. 2 - Thematic map of the most frequent keywords regarding geopolymers and adsorption from 2012 to 2022.



Source: the author

2.3 SYNTHESIS AND CHARACTERIZATION OF GEOPOLYMERS

GPs are inorganic polymers formed by the geopolymerization of aluminosilicate precursors with alkali or acid activation. This chemical reaction induces the formation of a three-dimensional solid structure in which Si atoms alternate with Al atoms in tetrahedral coordination, sharing all oxygen atoms (Davidovits, 2017, 1991). GPs can present highly porous amorphous or semicrystalline structures, similar to those found in zeolites (Duxson et al., 2007; Xu and Van Deventer, 2000). GPs exhibit outstanding physical, mechanical, thermal, and chemical properties (Komnitsas and Zaharaki, 2007). Moreover, they can be fabricated at temperatures below 100 °C from a wide range of raw materials including residues.

During geopolymerization, the activator solution promotes charging with metallic cations on the material's surface to compensate for the negative charge left by Al. There are two different routes for GP synthesis, either using alkaline (e.g., NaOH, KOH, LiOH, Ca(OH)₂, CsOH) or acid precursors (e.g., H₃PO₄, organic carboxylic acids) (Davidovits, 2017). The alkali route is the most frequently employed.

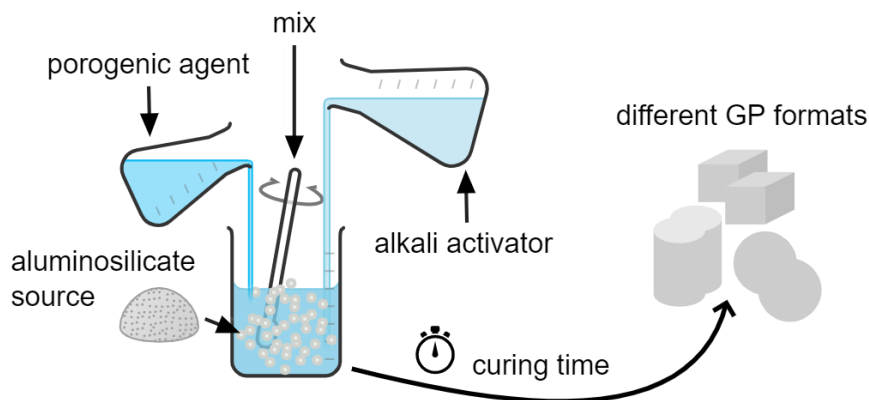
Metakaolin (MK) is a widespread source of aluminosilicate. However, some natural and industrial wastes present similar chemical compositions, which can totally or partially replace MK (De Rossi et al., 2019). Many works use residual raw materials, such as fly ash (FA) (Simão et al., 2021), waste glass (WG) (Toniolo et al., 2018), red mud (RM) (Geng et al., 2017), coal ultra-fine fly ash (CUFA) (Acisli et al., 2020), blast furnace slag (BFS) (Izquierdo et al., 2010), stone cutting (SC) (Simão et al., 2020). This approach reduces production costs and adds value to wastes.

The chemical, physical, and structural characteristics of geopolymers are directly related to raw materials, mix proportion, and curing conditions (Duxson et al., 2007). Thus, GP materials can be manufactured with tailored compressive strength, porous structure and surface area (De Rossi et al., 2019; Simão et al., 2020). In this regard, GPs are strong candidates for applications in separation processes involving membranes and adsorption.

2.3.1 Geopolymer synthesis

Fig. 3 shows a basic scheme for the synthesis of a porous GP. One or more aluminosilicate sources are dissolved by the action of the alkaline activator, forming silicate and aluminate monomers. At the same time, the porogenic agent is added for the formation of pores in the material. After mixing and homogenization, the paste is placed in molds and cured until the GP is produced.

Fig. 3 - Basic scheme for geopolymer synthesis (created in Chemix).



Source: the author

2.3.1.1 Raw materials of geopolymers

Many studies have reported the possibility of using residual materials for GP synthesis. The main reason is the valuation of waste and the reduction of the environmental impact of disposal in landfills. A potential precursor for the production of GPs must be rich in Si and Al. Table 1 shows that the chemical composition of alternative raw materials is diverse. Some, such as rice husk ash (RHA), have high percentages of SiO₂ (96.68%), while red mud (RM) has only 12.83% of the same oxide. Therefore, GPs are generally developed from a binary or ternary mixture to produce a suitable Si/Al ratio (Ren et al., 2021). According to Duxson et al. (2005), the molar composition of Si and Al source affects GP microstructural formation. For Si/Al ratios ≤ 1.4 , larger and interconnected pores are formed, while homogeneously distributed micropores are generated for Si/Al ratios ≥ 1.65 . To explain the change in microstructure, the authors correlated the variation of the silicate source with the alkali activator solution responsible for controlling the rate of structural reorganization.

Table 1 - Chemical composition of aluminosilicate sources for geopolymer synthesis.

| Oxides (wt.%) | CUFA | FA* | FA* | RHA | WG | RM | MK |
|--------------------------------|----------------------|----------------------|-----------------------|-----------------------|-----------------------|--------------------|---------------------|
| SiO ₂ | 55.34 | 34.00 | 25.34 | 96.68 | 70.50 | 12.83 | 54.40 |
| Al ₂ O ₃ | 29.39 | 13.50 | 6.05 | 0.29 | 3.20 | 20.26 | 39.40 |
| Fe ₂ O ₃ | 5.97 | 4.95 | 4.15 | 0.30 | 0.42 | 33.39 | 1.80 |
| Na ₂ O | 0.26 | 1.52 | 0.95 | 0.08 | 12.00 | 10.85 | - |
| K ₂ O | 4.21 | 5.49 | 5.84 | 1.36 | 1.00 | - | 1.0 |
| CaO | 1.20 | 16.50 | 36.72 | 0.99 | 10.00 | 0.87 | 0.10 |
| MgO | 2.22 | 3.07 | 3.61 | 0.30 | 2.30 | 0 | 0.1 |
| MnO | - | 0.45 | 0.42 | 0 | - | - | - |
| TiO ₂ | 1.23 | 0.65 | 0.60 | 0 | - | - | 1.5 |
| SO ₃ | <0.01 | 2.77 | 3.84 | - | - | 0.60 | - |
| P ₂ O ₅ | - | 1.11 | 4.70 | - | - | - | 0.1 |
| LOI | 2.07 | 14.3 | 5.12 | - | - | 2.28 | 2.7 |
| Ref. | Acisli et al. (2020) | Novais et al. (2019) | Novais et al. (2018b) | Barbosa et al. (2018) | Toniolo et al. (2018) | Geng et al. (2017) | Simão et al. (2021) |

* Two biomass fly ashes with different chemical compositions

Note: CUFA – Coal Ultrafine Fly Ash, FA – Fly Ash, MK – MetaKaolin, RHA – Rice Husk Ash, RM – Red Mud, WG – Waste Glass, LOI – Loss On Ignition.

The properties of geopolymers are dependent on the types of alkaline activators being used. Examples of activators include hydroxides such as NaOH and KOH or a mixture of both; sodium or potassium-based silicate solutions; and carbonates. However, a recent study demonstrated the possibility of using different alkaline activators derived from industrial and agricultural residues (Mohapatra et al., 2022).

2.3.1.2 *Porogenic agents*

Additives such as hydrogen peroxide (H_2O_2), aluminum powder, and soybean oil have been evaluated as pore-forming agents (De Rossi et al., 2019; Netto et al., 2020). Xu et al. (2018) found that H_2O_2 contents lower than 1% promoted pores with 0-1 mm in diameter, while higher H_2O_2 concentrations resulted in a decrease in tiny pores and an increase in the number of pores between 1 and 2 mm. Barbosa et al. (2018) compared the physical characteristics of GPs synthesized with and without soybean oil, and they concluded that the additive was responsible for increasing surface area (from 27 to 62 $\text{m}^2 \text{g}^{-1}$) and pore volume (0.13 to 0.36 $\text{cm}^3 \text{g}^{-1}$), and formed pores with larger diameters (9.1 to 14.3 nm). Novais et al. (2018a) evaluated different levels of aluminum powder as a pore-forming agent, and they found that it affected the number and volume of pores. Still, connectivity between the pores was attributed to the solid/liquid ratio. They also concluded that Al powder allows better control of pore size and distribution compared to H_2O_2 .

2.3.1.3 *Processing parameters*

Several factors affect the properties of GPs, such as the composition of aluminosilicate sources, particle size and distribution, degree of amorphization, water content, curing time, and temperature (Zribi et al., 2019). Many studies focused on the effect of GP curing conditions on pore formation (De Rossi et al., 2020, 2019; Trincal et al., 2022). Izquierdo et al. (2010) showed that open curing promotes the formation of highly porous solids with low strength when compared to curing in molds protected from contact with air. In addition, porosity was not homogenous but concentrated in the region with greater contact with air. Trincal et al. (2022) carried out an extensive

study on the influence of curing conditions on the porosity of GPs, and they found that pore distribution remains stable under autogenous conditions throughout curing time. Drying temperatures have significant effects on pore formation. Up to 40 °C, there was no change in mechanical strength, although pore size distribution started to be affected. When the temperature was raised to 60 and 105 °C, nano and microcracks were formed, increasing porosity and pore size (Izquierdo et al., 2010). Some works reported that increased temperature did not induce any mineralogical changes in GPs. The diffractograms revealed amorphous structures regardless of the evaluated temperature and the composition of the aluminosilicate source (Izquierdo et al., 2010; Zribi et al., 2019). However, curing under hydrothermal conditions at temperatures close to 100 °C led to the formation of zeolites (De Rossi et al., 2019; Qiu et al., 2015).

2.3.1.4 *Shaping of geopolymers*

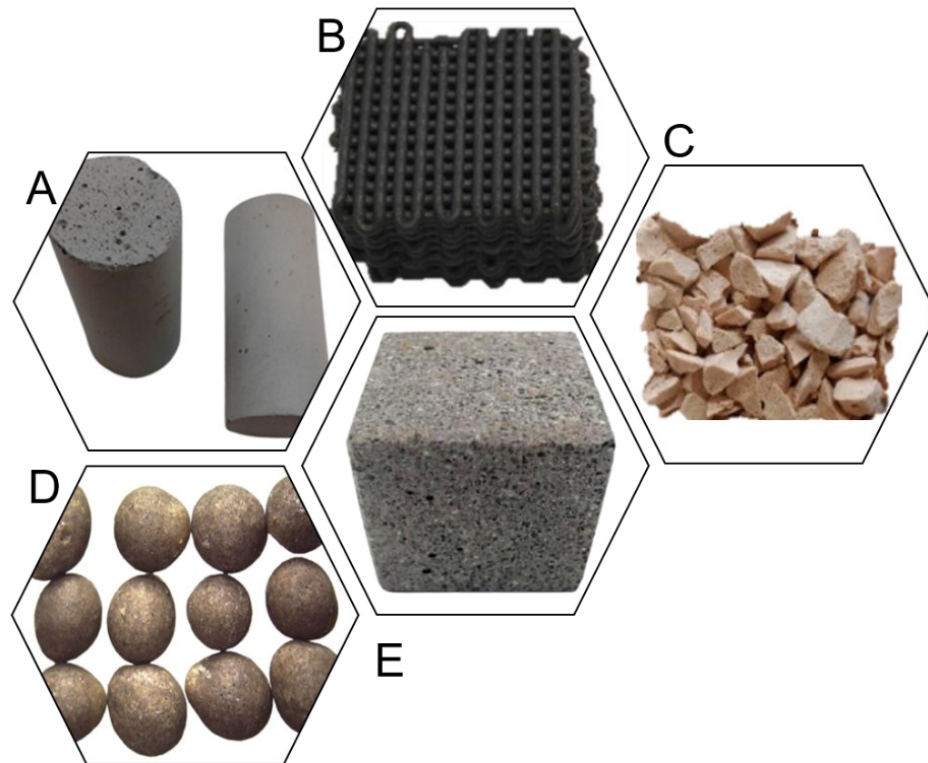
Geopolymers can be molded into different shapes (Fig. 4), such as monoliths (Novais et al., 2018b, 2016), spheres (Novais et al., 2019), blocks (Qiu et al., 2015; Z. Zhang et al., 2016) and tiny particles (Fumba et al., 2014; Ji et al., 2021). Nevertheless, most of the works involving adsorption grind GPs into small and medium particles (74-100 µm) (Fumba et al., 2014; Ji et al., 2021; Rossatto et al., 2020; Tome et al., 2021). The particle size of the adsorbent has a strong influence on the mass transfer of the adsorbate onto the solid surface, thus affecting adsorption. Fine particles have a larger surface area; therefore, powder adsorbents have greater adsorption capacity (Hosseini Asl et al., 2019). However, small particle size adsorbents pose a challenge to industrial applications in adsorption in fixed-bed columns. Alternatively, the adsorbent powder can be attached to supports or molded in porous ceramics, polymeric foams, and permeable bags (Z. Zhang et al., 2016).

Novais et al. (2018b) produced cylindrical discs of geopolymer concrete (GPC) (thickness of 3 mm; diameter of 22 mm, and length of 48 mm), which were submitted to endurance assays, and they exhibited distinct porosities. The GPC revealed high total porosity of 80.6 and 70.1%, respectively with the use of FA and MK. An advantage is that monolithic bodies could be used directly in packed beds, and easily handled after exhaustion of the adsorption capacity. Novais et al. (2019) also synthesized porous fly ash-based geopolymer spheres (GPS), with a diameter range from 2.6 to 2.9 mm). Their study aimed to reduce the particle size, expecting to increase the

surface area and, therefore, achieve higher adsorption capacity. Thus, they found that the spherical shape improved adsorbent performance and the GP application in wastewater treatment plants.

As reported by Zhang et al. (2022), the connection between pores in adsorbent materials allows the formation of structures with adequate porosity in monoliths that allow easy application in separation processes; thus, the development of GPs by extrusion, direct ink writing or 3D printing has been recently reported (Franchin et al., 2020; Oliveira et al., 2022). Oliveira et al. (2022) employed 3D printing to manufacture GPs in the form of a grid, maintaining preferential paths for the flow of the adsorbate, and increasing the permeability when compared to monoliths and packed beds. However, as for the adsorption capacity of 3D-printed porous geopolymers, there was a reduction in the adsorption rate, but this result was already expected since particle size is directly linked to the surface area and the sites available for sorption. Nevertheless, the easy reuse of the adsorbent makes the investigation of this new format very relevant. In addition, Franchin et al. (2020) concluded that direct ink writing allows the effective creation and customization of porous adsorbents with optimal properties.

Fig. 4 - Geopolymer shapes: cylindrical (A), 3D-printed (B), granulated (C), spherical (D), and block (E)



Source: Novais et al. (2019, 2016); Oliveira et al. (2022); Sanguanpak et al. (2021); M. Zhang et al. (2016)

2.3.2 Geopolymer characterization

Adsorption is a mass transfer process; for this reason, knowledge of the characteristics of the adsorbent is important to understand how interaction occurs and to elucidate the mechanisms involved between the adsorbent and the adsorbate (Sanguanpak et al., 2021). Thus, this section discusses relevant characterization techniques and their implication.

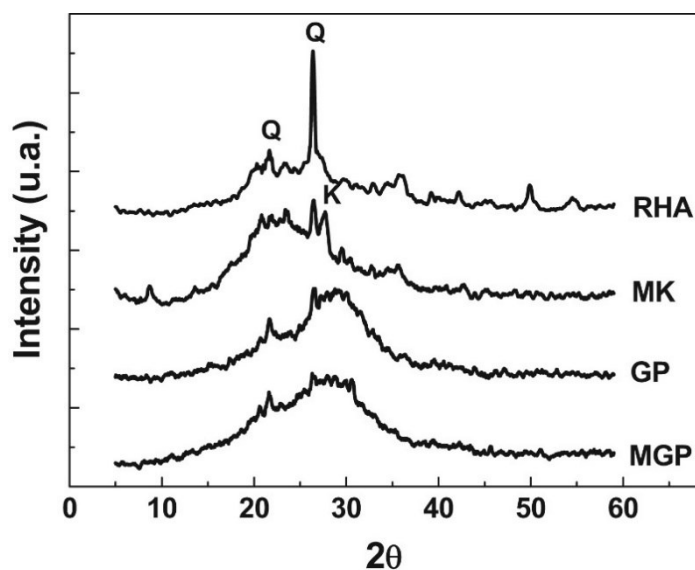
2.3.2.1 *Microstructural analysis*

The microstructure of GPs has been evaluated using scanning electron microscopy (SEM). Alternatively, optical microscopy can be applied to check morphological aspects. Using textural analysis, researchers can identify the formation of an amorphous structure that is typical of geopolymers (Khan et al., 2015b) or

crystalline structures that are common in zeolites (De Rossi et al., 2019). For example, Geng et al. (2017), when analyzing GP micrographs, concluded that starting materials with finer grain sizes, combined with thermal curing conditions, resulted in the formation of low-porosity dense structures. Khan et al. (2015a) managed to observe the disintegration of large particles into nanoparticles, considering different formulations and cure times. As the micrographs are scaled, pore size and pore distribution can be approximated by using image analysis software (Novais et al., 2019).

X-ray diffraction (XRD) provides information about the phase composition (amorphous and crystalline) of the geopolymer. Some characteristic peaks of raw materials disappear during geopolymerization, while amorphous GP-related structures arise. Barbosa et al. (2018) found very sharp peaks of crystalline silica (quartz) in rice husk ash, which were decomposed and did not appear in the amorphous structure of the GP (Fig. 5). An in-depth analysis of the curing conditions associated with XRD allowed De Rossi et al. (2019) to conclude that quartz, calcite, and muscovite (present in the raw materials) remained in the GPs cured at room temperature, while faujasite and P zeolites were formed in hydrothermal curing. Other works have also reported similar results, for example, the study of Qiu et al. (2015), which reported that GP formed from fly ash in a hydrothermal process resulted in the formation of NaP zeolites. Novais et al. (2018a) evaluated different Al contents for the production of GP and concluded that Al did not affect the mineralogical composition.

Fig. 5 - XRD patterns of RHA (Rice Husk Ash), MK (Metakolin), GP (Geopolymer), and MGP (Mesoporous Geopolymer).



Source: Barbosa et al. (2018)

2.3.2.2 Physical analysis

Knowledge of the physical properties of adsorbent material is fundamental. High surface areas, porosity, and pore volume are desirable and contribute to high sorption capacity. Table 2 shows the main physical characteristics of GPs developed from different raw materials. There is a wide range of adsorbent surface areas (8.2 to 90.3 m² g⁻¹) and pore volumes (0.02 to 0.24 cm³ g⁻¹). Micro and mesoporous adsorbents are found (0.1 nm to 14.4 nm). As mentioned previously, high surface areas and pore volumes favor the removal of adsorbates, but adsorption mechanisms are complex. The GP produced by Netto et al. (2020) had an area of approximately 43 m² g⁻¹, which is small in comparison to other adsorbents. However, when applied to the removal of acid red 97 dye, it showed a high affinity, resulting in an adsorption capacity of 1814 mg g⁻¹.

Thermogravimetric analysis (TGA) is a technique used to assess the thermal stability of samples and volatilized fractions with increasing temperature. According to Khan et al. (2015b), an adsorbent must support high temperatures for effective regeneration and reuse. Two studies reported GP stability at 800°C, showing a mass loss of 9.5% (Khan et al., 2015b) to 14% (Khan et al., 2015a). Furthermore, TGA allows

identifying which components degrade at high temperatures, corroborating to explain the formation of GPs (Tome et al., 2021).

Mechanical properties are a critical physical indicator that raw materials react to obtain a geopolymer. At a high rate of geopolymerization, an increase in mechanical properties is expected. In addition, mechanical properties are necessary for a stable and structured material that will be used for adsorption, such as a spherical or monolithic porous sample. To increase the porosity and consequently decrease the density of these geopolymer samples, some strategies could be used with different foaming agents (Novais et al., 2020).

Table 2 - Sources used for the synthesis of geopolymers and their physical characteristics.

| GP Sources | Surface area (m ² g ⁻¹) | Average pore size (nm) | Pore volume (cm ³ g ⁻¹) | Reference |
|--|--|------------------------|--|------------------------|
| MK, BS, SO, H ₂ O ₂ , Fe ₃ O ₄ , NaOH | 19.5 | 14.4 | 0.04 | Hua et al. (2020) |
| MK, BS, SO, H ₂ O ₂ , ZVI, NaOH | 42.9 | 4.9 | 0.05 | Netto et al. (2020) |
| MK, RHA, SO, KOH | 62.0 | 14.3 | 0.36 | Barbosa et al. (2018) |
| MK, BS, SO, H ₂ O ₂ , Fe ₃ O ₄ , NaOH | 53.4 | 14.1 | 0.19 | Rossatto et al. (2020) |
| MK, RHA, KOH | 27.0 | 9.1 | 0.13 | Barbosa et al. (2018) |
| FA, S, SS, NaOH | 90.3 | 8.4 | 0.21 | Khalid et al. (2018) |
| FA, S, SS, NaOH | 76.6 | 12.5 | 0.24 | Khalid et al. (2018) |
| MK, SS, NaOH | 8.2 | 10.5 | 0.02 | Lan et al. (2019) |
| FA, H ₂ O, NaOH | 56.0 | - | 0.14 | Li et al. (2006) |
| VA, SS, C ₃ H ₆ O, NaOH | 74.5 | - | 0.06 | Tome et al. (2021) |
| VA, SS, C ₃ H ₆ O, H ₃ PO ₄ | 42.7 | - | 0.15 | Tome et al. (2021) |
| MK, Al ₂ O ₃ , H ₂ O H ₃ PO ₄ | 33.4 | 8.6 | 0.07 | Khan et al. (2015b) |
| MK, S, SiO ₂ -sol, KOH | 44.8 | 0.1 | 0.12 | Feng et al. (2021) |
| CUFA, H ₂ O, NaOH | 47.4 | 9.8 | 0.16 | Acisli et al. (2020) |

Note: BS – Biogenic Silica, CUFA – Coal Ultrafine Fly Ash, FA – Fly Ash, M – Magnetite, MK – MetaKaolin, RHA – Rice Husk Ash, S – Slag, SO – Soybean Oil, SS – Sodium Silicate, VA - Volcanic Ash, ZVI – Zero-Valent Iron.

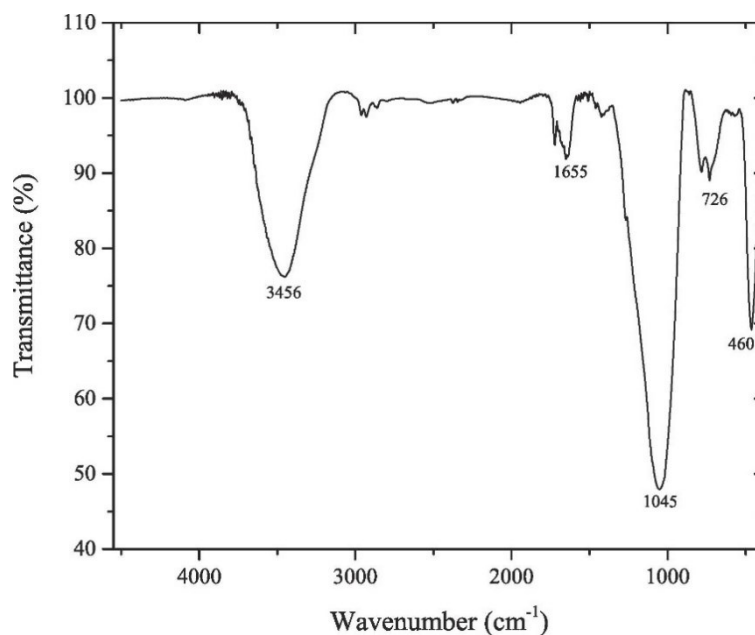
2.3.2.3 Chemical analysis

The chemical composition of the GPs can be disclosed by different techniques. Fourier Transform InfraRed spectroscopy (FTIR) is the most used to identify functional groups, while the combined use of Energy Dispersive spectroscopy (EDS) and Scanning Electron Microscopy (SEM) allows the semiquantitative determination of the chemical composition of the GP sample.

FTIR is used to identify the surface functional groups of raw materials and products. Within the spectrum from 4000 to 400 cm^{-1} , characteristic vibrations of the main functional groups of GPs can be seen. Stretching around 3400 cm^{-1} and flexions at 1640 cm^{-1} can be associated with the O-H group present in GPs because of adsorbed water. Elongated bands close to 1035 cm^{-1} indicate the occurrence of geopolymerization since they are associated with asymmetric vibration of T-O-T (where T can be Si or Al). Another group that suggests geopolymer formation is Si-O-T (T=Si or Al), which is found in symmetric and asymmetric vibrations close to 700 cm^{-1} . Peaks in the 460 cm^{-1} regions are expected, as they are associated with the presence of Al-O/Si-O (Hua et al., 2020; Rossatto et al., 2020). These characteristics were found in all GPs synthesized with different raw materials and alkaline activating agents, as shown in Fig. 6.

An in-depth analysis of FTIR allows the extraction of relevant information. For example, Barbosa et al. (2018) correlated large and overlapping absorption bands to the amorphous character of the compounds and found that the presence of the foaming agent (soybean oil) did not change the infrared spectrum. They finally noticed that a small displacement of the GP band position on basis of the raw materials (MK and RHA) is caused by alkaline activation. Khan et al. (2015a) also demonstrated that the change in absorption peaks helps to understand how GPs are formed. Furthermore, when FTIR is used on GPs after adsorption, characteristic peaks of the adsorbate should appear in the spectrum. In the works published by Novais et al. (2019, 2018b), the appearance of a band was demonstrated in 1610 cm^{-1} after MB dye removal; this elongated peak is related to the aromatic ring. There were other vibrations associated with methylene (1335, 1355, and 1410 cm^{-1}), confirming the adsorption of the dye in the GP.

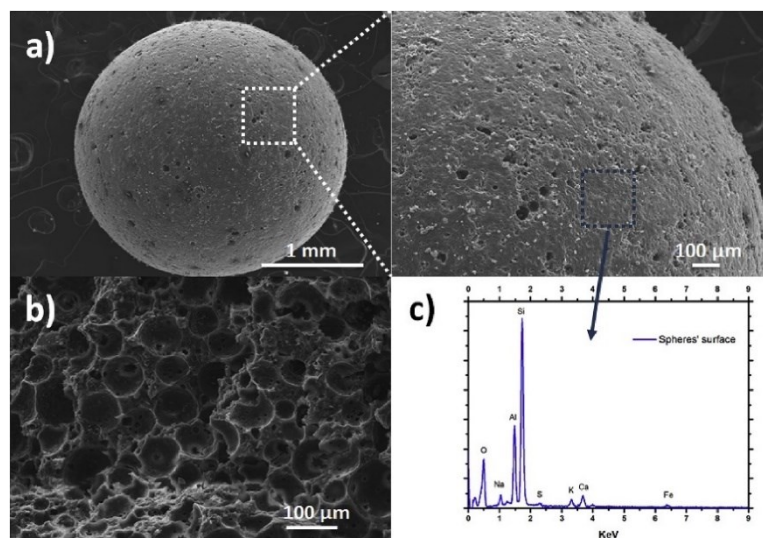
Fig. 6 - FTIR spectra of geopolymer adsorbent.



Source: Hua et al. (2020)

The EDS spectra used to characterize GPs can show the different chemical compositions depending on the nature of the raw materials. Chemical elements such as Al, Si, and O are prevalent in GPs (Jin et al., 2021), but other elements can appear to a greater or lesser extent, depending on the aluminosilicate source. A GP produced with MK had Na as the third most abundant element, while Ca appeared with greater intensity (Novais et al., 2018b). A typical behavior during geopolymerization is efflorescence resulting from a chemical reaction between alkali activators and atmospheric CO₂ (Simão et al., 2021). When NaOH is used, Na diffuses to the surface of the GP during curing. This behavior can be seen (Fig. 7) through EDS performed in the bulk and at the surface of the GP sample, with a predominance of Na at the latter (Novais et al., 2019). The interpretation of the kinetic modeling combined with SEM/EDS results can help confirm the influence of chemisorption on the process (Khalid et al., 2018). Performing EDS on samples after desorption can also help understand the results. For example, Jin et al. (2021) found the presence of Ni²⁺ in GP; however, they did not find evidence of MB dye, demonstrating that the dye was efficiently desorbed.

Fig. 7 - SEM micrographs of the (a) spheres' surface and (b) inner part after regeneration of the adsorbent and, (c) the EDS spectrum of the surface.



Source: Novais et al. (2019)

2.4 DYE ADSORPTION

As discussed in the previous section, different raw materials and synthesis methods enable the development of porous GPs with good adsorptive properties. The application of geopolymers as adsorbents in the removal of dyes is discussed below, taking into account the studied dyes, the adsorption mechanisms, and also the recovery of GPs after adsorption.

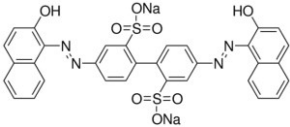
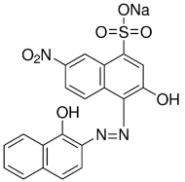
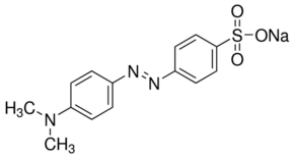
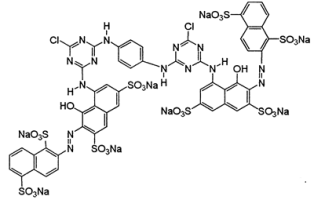
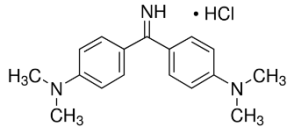
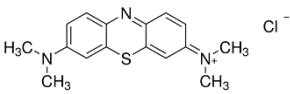
2.4.1 Dyes removed by adsorption

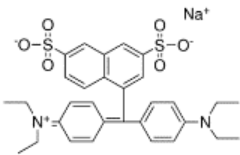
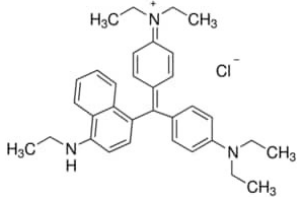
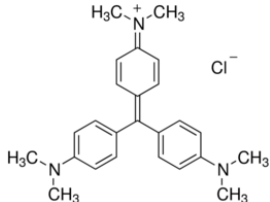
This Section is limited to dyes found in research papers using GP for adsorptive removal (Table 3), organized by chromophore groups. The most used dye is methylene blue (MB). Regarding applications, the thiazine and diphenylmethane classes are directed to the biomedical field. Moreover, azo and triarylmethane dyes are used in the textile industry owing to their strong solidity and intense color.

Azo is the most important class of dyes, found in over 70% of commercial dyes. Azo dyes have at least one azo group ($-N=N-$) but can contain two or more. The azo group is attached to two radicals, and at least one is aromatic. Thiazine is classified as a sulfur dye. MB is a relatively simple substance and is used as a model molecule for comparison with new adsorbents. Diphenylmethane is characterized by having two

phenyl groups in place of hydrogen in the methane molecule. Triarylmethane is a synthetic organic dye that contains the triphenylmethyl radical (Waring and Hallas, 1990). Nevertheless, in the revised papers the dyes are rarely classified according to their chemical structure. The chromophore groups and the auxochromes are not usually mentioned. The common classification adopted is the method of dyeing (dispersed, direct, reactive, acid, etc.).

Table 3 - Dyes removed by adsorption using geopolymers.

| Dye | Color Index | Molecular structure | Chromophore group | λ_{\max} (nm) | Molecular weight (g mol ⁻¹) | Reference |
|--------------------------|-------------|--|-------------------|-----------------------|---|-----------------------|
| Acid Red 97 (AR97) | 22890 |  | Azo | 498 | 698.6 | Netto et al. (2020) |
| Eriochrome Black T (EBT) | 14645 |  | Azo | 600 | 461.4 | Tome et al. (2021) |
| Methyl Orange (MO) | 13025 |  | Azo | 507 | 327.3 | Selkälä et al. (2020) |
| Procion Red (PR) | - |  | Azo | 543 | 1774.2 | Hua et al. (2020) |
| Basic Yellow 2 (BY2) | 41000 |  | Diphenylmethane | 432 | 303.8 | Acisli et al. (2020) |
| Methylene Blue (MB) | 52015 |  | Thiazine | 664 | 319.8 | Novais et al. (2018b) |

| | | | | | | |
|---------------------------|-------|--|----------------|-----|-------|-----------------------|
| Acid Green 16 (AG16) | 44025 |  | Triarylmethane | 640 | 616.7 | Hua et al. (2020) |
| Basic Blue 7 (BB7) | 42595 |  | Triarylmethane | 616 | 514.1 | Akar et al. (2021) |
| Methyl Violet 10B (MV10B) | 42555 |  | Triarylmethane | 590 | 408.0 | Barbosa et al. (2018) |

Source: National Center for Biotechnology Information (pubchem.ncbi.nlm.nih.gov/)

In general, dyes are organized regarding the presence of aromatic rings, so a relationship with the molecular weight can be established. Compounds with a higher number of arenes have high molecular weight and larger sizes. This correlation can be seen in MB and PR dyes. Dyes with a higher molecular structure are more difficult to remove in adsorptive processes, as demonstrated by Hua et al. (2020) and Tome et al. (2021).

2.4.2 Removal efficiency and adsorption mechanisms

Table 4 shows that the adsorption capacities (q_e) of different dyes range from 0.3 to 1814 mg g⁻¹. These results are directly linked to the characteristics of GPs and their affinity with dye molecules. For example, a magnetic geopolymer developed by Hua et al. (2020) was more effective in removing triarylmethane (AG16) and azo (PR) because of dye characteristics such as molecule size. Also, the synthesis of GP with alkaline activation is more effective in removing EBT (251 mg g⁻¹) and MB (952 mg g⁻¹) when compared to activation with H₃PO₄ ($q_{e\text{EBT}} = 39.1$ mg g⁻¹, $q_{e\text{MB}} = 22.9$ mg g⁻¹) (Tome et al., 2021).

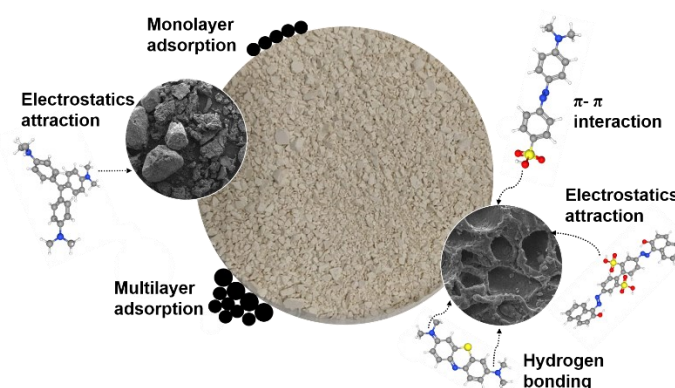
Operating conditions can make it difficult to scale up a separation process; hence, fast kinetics is desirable. Some studies had satisfactory results for dye removal in up to 60 min of adsorption (Akar et al., 2021; Tome et al., 2021), while others took more than 5 h to reach equilibrium (Acisli et al., 2020; Novais et al., 2019), making the process unfeasible. The adsorbent dosage is also an essential condition because it is linked to q_e . While some works use low concentrations of GPs (up to 2 g L⁻¹) (Hua et al., 2020; Netto et al., 2020), others need 16 g L⁻¹ (Khan et al., 2015b) or 20 g L⁻¹ (Acisli et al., 2020), which results in lower sorption capacities and increasing adsorbent costs.

Table 4 - Dye adsorption capacity (q_e) of geopolymer adsorbents

| Dye | pH | Temperature (°C) | time (min) | GP dosage (g L ⁻¹) | q_e (mg g ⁻¹) | Reference |
|-------|------|---------------------|---------------|-----------------------------------|-----------------------------|------------------------|
| AR97 | 3 | 45 | 180 | 0.5 | 1814.0 | Netto et al. (2020) |
| PR | 3 | 55 | 300 | 1 | 41.8 | Hua et al. (2020) |
| MO | 2.5 | 25 | 40 | 0.4 | 0.3 | Fumba et al. (2014) |
| AG16 | 3 | 55 | 300 | 1 | 187.5 | Hua et al. (2020) |
| | 2 | 55 | 30 | 0.75 | 400.0 | Rossatto et al. (2020) |
| MV10B | 4.5 | 25 | 120 | 1.5 | 76.9 | Barbosa et al. (2018) |
| EBT | - | 50 | 30 | 2 | 51.0 | Tome et al. (2021) |
| | - | 50 | 30 | 2 | 9.1 | Tome et al. (2021) |
| BB7 | 4.4 | 25 | 60 | 2.8 | 6.1 | Akar et al. (2021) |
| BY2 | 9.85 | 50 | 300 | 20 | 3.5 | Acisli et al. (2020) |
| MB | - | 25 | 0 | 2 | 952.0 | Tome et al. (2021) |
| | - | 25 | 0 | 2 | 22.9 | Tome et al. (2021) |
| | 4.5 | 25 | 1800 | - | 15.4 | Novais et al. (2018b) |
| | 4.8 | 28 | 180 | 16 | 3.0 | Khan et al. (2015b) |
| | 10 | - | 10 | 7 | 19.8 | Jin et al. (2021) |
| | 4.5 | - | 1440 | 7.5 | 45.8 | Novais et al. (2019) |

Understanding the mechanisms that control adsorption is an important task, but it requires an in-depth analysis of the contribution of each interaction and/or chemical bond in the adsorptive process (Pan and Xing, 2008). Many studies use theoretical models to explain the mechanisms, such as adsorption isotherms, kinetics models, and statistical or empirical equations (Fig. 8).

Fig. 8 - Schematic illustration of MB adsorption mechanisms onto geopolymer.



Source: the author

Through adsorption isotherms (classified as type I), the removal of BY2 was attributed to chemical bonds originating from a monolayer on the surface of the GP (Acisli et al., 2020). According to Jin et al. (2021), adsorption performance in MB removal was controlled by the ion exchange of Na^+ present in GPs and water in alkaline conditions, allowing the exposure of a high number of negative charges. This finding suggests that the chemisorption mechanism controls the process, a result that was confirmed by the pseudo-second-order kinetic model. Chemisorption is usually governed by ionic or covalent bonds (Crini, 2006).

However, Hua et al. (2020) developed a statistical model to interpret the dye adsorption mechanism, considering the formation of multilayers and different interaction energies instead of using classical pseudo-first and second-order models. As a result, the authors conclude that the dye adsorption mechanism was energetically controlled by physical interactions, such as electrostatic and Van der Waal forces (Crini, 2006). The physical adsorption mechanisms are directly involved with the electrical charge of the adsorbent and the adsorbate, thus, the positively charged GPs have a greater power to attract acid dyes or other dyes in acidic media (Açışlı et al., 2022). Some studies listed in Table 4 confirm this analysis, e.g., the work by Netto et al. (2020) that evaluated the removal of AR97 in a solution with pH 3 and obtained an extremely satisfactory result for adsorption capacity, 1814 mg g^{-1} . Similarly, other studies that used solutions in an acidic medium (pH 3) resulted in good removal of PR and AG16 dyes (Hua et al., 2020). Li et al. (2022) reinforce that adsorbent selectivity is linked to the characteristics of the adsorbate; in their study, the geopolymer activated with NaOH but modified with HNO_3 was highly efficient in removing cationic dyes in comparison to anionic ones.

One of the most important and elementary analyses that must be carried out to understand the mechanisms involved in adsorption processes is to check the average pore size and molecular diameter of the adsorbate. After all, this analysis can clarify if the molecule can be adsorbed in the pores or just on the external surface. However, it is difficult to obtain information about the size of several molecules, for example, those of dyes. In the work by Hua et al. (2020), there was a greater adsorption capacity for the dye AG16 (180 mg g^{-1}) when compared to PR (45 mg g^{-1}). To understand this behavior, the authors found that the molecular weight of PR is $2.8\times$ higher than that of AG16 (see Table 3). Consequently, the size of the azo dye is also

much larger. Thus, they concluded that the adsorption of the PR occurred only on the external surface of the GP.

2.4.3 Desorption and regeneration

The reuse of the adsorbent after saturation is essential to ensure the economic viability of the process. The adsorbent can be recovered either by desorption - a solvent is used to promote the separation of the adsorbate from the solid or by regeneration - in which the adsorbent is treated at temperatures that promote the degradation of the adsorbate.

The desorption of dyes can be more difficult when compared to other adsorbates, such as metals, especially when the controlling mechanism is chemisorption (Jin et al., 2021). Furthermore, porosity and the source of aluminosilicates are related to dye retention capacity (Novais et al., 2018b). GPs with higher porosities showed higher percentages of dye leaching in the aqueous phase. Moreover, it was found that GPs based on MK have a greater affinity with MB dye while GPs produced from FA had lower dye retention (Novais et al., 2018b). Thus, a solvent must be able to break the bonds between a dye and a GP. Acid washing is commonly used to desorb cationic dyes. However, Jin et al. (2021) did not achieve satisfactory results using HCl to separate the MB dye. Another strategy is to use acetone; as demonstrated by Akar et al. (2021), triarylmethane (BB7) desorption was close to 100% in 20 successive cycles.

Regarding thermal regeneration of adsorbent geopolymers, the most used condition is the calcination of GPs at 400 to 500 °C for 2 h (Netto et al., 2020; Rossatto et al., 2020). Still, their thermal stability needs to be evaluated before the selection of the thermal conditions, as explained by Khan et al. (2015b). The GP monoliths developed by Novais et al. (2018b) showed satisfactory regeneration results after thermal treatment, increasing the initial adsorption capacity from 15.4 to 20.5 mg g⁻¹. Similar results have been reported in other studies (Khan et al., 2015b; Novais et al., 2019). GPs are normally cured at temperatures below 100°C. Thus, calcination causes the dehydration of bound and interstitial water molecules, promoting the opening of more active sites and increased porosity (Khan et al., 2015a). This way, the adsorbent can be reused for many cycles and enhances economic viability (Khan et al., 2015b). For example, Rossatto et al. (2020) managed to maintain an adsorption capacity close

to 120 mg g⁻¹ for 4 cycles, in agreement with Netto et al. (2020), who maintained q_e around 1800 mg g⁻¹, and found a 50% decay in the 10th cycle.

2.5 CHALLENGES AND PROSPECTS

Considering recent findings on the use of porous geopolymers for dye adsorption, some gaps still need to be explored and elucidated. To shed light on relevant questions, some references and readings can contribute new ideas for application in dye removal, as follows.

i) How to increase the number of active sites for adsorption?

The use of additives for pore formation focuses on H₂O₂, soybean oil, and alumina powder. However, when GP is exposed to an acid attack, the three-dimensional structure of -Si and -Al can be disrupted, increasing porosity. The study by Chen et al. (2022) revealed that contact with HNO₃ resulted in a 20× increase in surface area.

ii) Can functionalization improve the adsorptive properties of the material?

Regarding functionalization, some compounds can be grafted to allow the insertion of functional groups into the structure of the adsorbent, and potentiate chemical bonds with the adsorbate (Chen et al., 2022) significantly increasing adsorption capacity (Huang et al., 2017).

iii) Are geopolymer composites an interesting strategy?

Adsorbent composites have also aroused great scientific interest because the properties and characteristics of different materials can be combined into a single adsorbent. As reported by Chen et al. (2021), geopolymerization with alkali activation on activated carbon promoted a 2.25× increase in CO₂ adsorption when compared to single materials.

iv) What are the advantages of 3D printing geopolymeric monoliths?

The geopolymer shape control represents a great technical advantage for new adsorbents. Three-dimensional printing can create paths for the adequate flow of the adsorbate and enable the generation of structures with connectivity between the pores, enhancing the material features for application in continuous-flow adsorption systems (Oliveira et al., 2022).

v) Is the same geopolymer capable of efficiently removing dyes with different ionic charges?

Another challenge is to synthesize adsorbents capable of efficiently removing anionic and cationic dyes. Particularly, Tome et al. (2021) proposed to do this evaluation, concluding that the electrostatic attractive forces control the adsorption. Nevertheless, a suitable adsorption capacity was obtained for both dyes.

vi) Are geopolymers economically competitive with activated carbon?

Finally, owing to the growing interest in the development of adsorbent geopolymers, an economic evaluation of the costs of the synthesis would be of great scientific interest. This is especially the case when comparisons are made to activated carbon, which is the most applied adsorbent in industrial effluent treatment plants.

2.6 CONCLUSIONS

Materials with high concentrations of Al and Si are potential sources to produce geopolymers. Thus, several industrial and agricultural residues can be used, but they require proper control of the molar composition and an adequate activating agent. In addition, for application as an adsorbent, the formation of pores is a relevant factor. In this regard, the use of additives such as H₂O₂ and soybean oil proved to be efficient, providing an increase in the surface area. The main functional groups found in GPs involve Si and Al. The addition of the porogenic agent does not change chemical composition, while the alkaline agent causes a small displacement of the bands. Through analyses of the mineralogical composition of samples cured under different conditions, zeolites and geopolymers were formed.

Most of the studies focused on the evaluation of the removal of methylene blue, while triarylmethanes and azo dyes are little explored, even though they have robust applications in the textile sector. The molecules are structured with the presence of several aromatic rings. Therefore, the size and molecular weight increase, hindering adsorption in the micropores. The characteristics of the geopolymers strongly influence the adsorption capacity of the dyes and alkaline activation was more effective when compared to its acid counterpart. Some studies showed promising results, with high rates of removal and favorable kinetics. For the reuse of GPs, the raw materials and pore distribution are linked to the desorption capacity of dyes. However, a more appropriate strategy is regeneration. Calcination at 500 °C promotes the degradation of the adsorbed molecule and possibly opens new active sites, allowing reuse in successive adsorption cycles.

Currently, the adsorption processes in the textile industries for color removal use activated carbon as an adsorbent; however, the analysis of the results shows that geopolymers are materials with desirable properties and with real potential for application in wastewater treatment systems.

CHAPTER III

In Chapter III, the experimental methods and results of the research are explored and discussed. The effect of changes in the geopolymer structure caused by acid attack and calcination are discussed, as well as the kinetic and thermodynamic behavior involved in the adsorption of dyes. This chapter is part of a research article that will be submitted for publication in the Journal of Cleaner Production, with the title *Acid attack followed by calcination to develop regenerable geopolymers for azo dye adsorption*².

3 GEOPOLYMER DEVELOPMENT AND APPLICATION FOR DYE ADSORPTION

3.1 INTRODUCTION

Geopolymers (GPs) are materials of great interest to the scientific community, with applications in several sectors, such as civil construction and more recently in catalytic and separation processes. GPs are obtained from aluminosilicate minerals, which in the presence of a strong alkaline agent are dissolved in $[\text{SiO}_4]^{4-}$ and $[\text{AlO}_4]^{5-}$ monomers that are bonded by oxygen atoms, forming an amorphous or semi-crystalline three-dimensional structure (Davidovits, 1991; M. Zhang et al., 2016).

Acid attack on cementitious matrices and especially GPs causes deterioration of the structure of aluminosilicates. In some cases, depolymerization can promote the formation of zeolites (Bakharev, 2005). Zhang et al. (2016) evaluated how the changes in the structure of the GP promoted by H_2SO_4 occur over 120 days. They noticed that, on the first day, there was a drastic decrease in the flexural strength, suggesting the appearance of cracks in the material, as proven by the SEM, and reinforced by the standards of XRD that demonstrated the dissolution of geopolymeric gels. In a recent study, Chen et al. (2022) were able to elucidate how pore formation occurs in GPs treated with HNO_3 , revealing that Si-O-Al bonds are broken by acid, forming Si-OH groups. This result is attributed to dealumination and desilicization, forming micro-cracks and pores in the GP, therefore the surface area had a jump from 21 to 412 $\text{m}^2 \text{g}^{-1}$.

² Article that will be submitted for publication

Calcination after geopolymerization has also shown an increase in the specific area of the adsorbents. Pan et al. (2023) studied the effect of calcination temperature (200-1000 °C) on the physical properties of GP, noting that the surface area accompanied the increase in temperature. The increase in the available area did not reflect the improvement of the adsorption capacity. However, there is still no agreement that calcination has a positive effect. Tian et al. (2022) found a decrease in the surface area with calcination, concluding that the increase in temperature removed the adsorbed water and promoted the formation of mesopores.

Thus, it is clear that the effect of changes in the structure of GPs needs to be extensively investigated. As a pioneering work, this work aims to evaluate the joint effect of acid attack and calcination in the development of a geopolymer with high porosity and surface area for the adsorption of azo dyes.

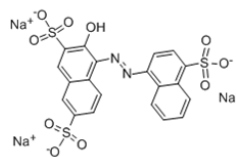
3.2 EXPERIMENTAL

3.2.1 Materials

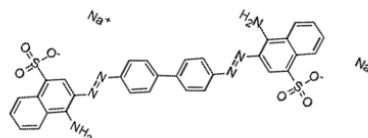
Metakaolin (MK, Imerys[®], 52.84 wt.% SiO₂, 43.31 wt.% Al₂O₂,) with mean particle of 1.37 μm was used as an aluminosilicate source while sodium hydroxide (NaOH, Neon) and neutral sodium silicate (SS, Quimidrol, 10.8 wt.% Na₂O, 34.20 wt.% SiO₂ and 55.0 wt.% H₂O) solutions were used as alkaline activating agents. Sulfuric acid (H₂SO₄, 98%, Synth) and phosphoric acid (H₃PO₄, 85% Synth) was used to open pores in the material. The following dyes were used: acid red 27 (AR27), direct red 28 (DR 28) and reactive red 194 (RR194), that has an anionic charge, and dispersed red 343 (DiR343), which is non-ionic. The structure of the respective molecules and other characteristics are described in Fig. 9.

Fig. 9 - Characteristics of the azo dyes used in the adsorption tests of this work.

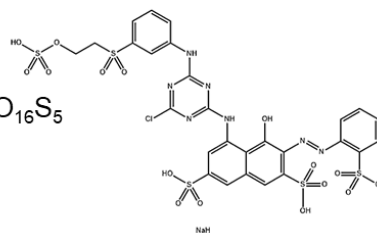
Name: Acid Red 27
 Color Index: 16185
 Molecular Formula: $C_{20}H_{11}N_2Na_3O_{10}S_3$
 Molecular Weight: 604.5 g mol^{-1}
 Wavelength: 520 nm



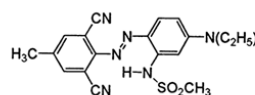
Name: Direct Red 28
 Color Index: 22120
 Molecular Formula: $C_{32}H_{22}N_6Na_2O_6S_2$
 Molecular Weight: 696.7 g mol^{-1}
 Wavelength: 498 nm



Name: Reactive Red 194
 Color Index: 18214
 Molecular Formula: $C_{27}H_{18}ClN_7Na_4O_{16}S_5$
 Molecular Weight: 984.2 g mol^{-1}
 Wavelength: 539 nm



Name: Disperse Red 343
 Color Index: 343
 Molecular Formula: $C_{20}H_{22}N_6O_2S$
 Molecular Weight: $4254.5 \text{ g mol}^{-1}$
 Wavelength: 584 nm



Source: the author

3.2.2 Geopolymer preparation

Initial tests were carried out to determine the minimum amount of Na_2SiO_3 for geopolymerization, avoiding excess alkaline activator. Thus 48 g of Na_2SiO_3 , 24 g of NaOH (8 M), 4 g of distilled water, and 80 g of MK were mixed at 250 rpm for 10 min in a propeller stirred (IKA, RW20). This mixture resulted in a molar ratio of $SiO_2/Al_2O_3 = 2.87$. The slurry was placed in 5 cm square molds and cured at room temperature for 24 h. Afterward, the geopolymer block was ground. The samples were washed with hot water until no change in the pH of the suspension was observed to remove excess alkali and dried in an oven (50 °C for 12 h) to remove moisture. The geopolymer material received the name GP.

3.2.3 Geopolymer modification

Initial tests were carried out with H_2SO_4 and H_3PO_4 to observe which acid would be able to promote greater adsorption efficiencies, as well as the calcination or not of GP was evaluated. For this purpose, the GP was placed in contact with the acids,

following a 1:1 ratio (m/v) between the GP and the acid, and kept for 12 h at 50°C. To assess whether calcination would bring positive effects, some samples of the material after contact with the acid were calcined in a muffle furnace at 500°C for 120 min. As a response to these tests, adsorption tests were carried out using 5 g L⁻¹ of the adsorbent produced and 15 mg L⁻¹ of DR28, being kept in agitation for 120 min at 30°C.

Confirming the beneficial effect on adoption, the two strategies (acid attack and calcination) were used to create pores in the GP. Thus, the concentration of H₂SO₄ and the calcination temperature were the factors investigated in the Central Composite Rotatable Design (CCRD) 2² design (Table 5), while the adsorption capacity (*q_e*) of modified GP and dye removal (R) of DR 28 was the response variable.

Table 5 – Factors and levels of the CCRD 22 experimental design matrix.

| Factors | Levels | | | | |
|------------------------------------|--------|-----|-----|------|-------|
| | -1.41 | -1 | 0 | +1 | +1.41 |
| H ₂ SO ₄ (%) | 0 | 4.4 | 15 | 25.6 | 30 |
| Calcination (°C) | 200 | 259 | 400 | 541 | 600 |

First, the GP was placed in contact with H₂SO₄ (concentration determined by CCRD design), maintaining a 1:1 ratio (m/v) between the material and the acid, according to preliminary tests. The mixture was dehydrated for 12 h in an oven at 50 °C followed by calcination in a muffle furnace (EDG, 3000 3P) with a constant heating rate of 10 °C min⁻¹ up to the set temperature (determined by CCRD design), remaining for 120 min. Afterward, the solid particles were washed with hot water until no change in the pH of the suspension was observed to remove excess acid and dried in an oven (50 °C for 12 h) to remove moisture (Chen et al., 2022). The GPs were manually sieved with a pestle and a particle size of <425 μm was used after granulometric separation.

The CCRD experimental data were statistically analyzed using the software Statistica 12, with 95% confidence (*p* < 0.05). Analysis of variance (ANOVA) and Fischer's F test were used to validate the mathematical models.

To evaluate the efficiency of the modified GP, batch adsorption tests were carried out to remove the dye. 5 g L⁻¹ of the GP was placed in contact of DR 28 dye aqueous solutions (200 mg L⁻¹) and constantly stirred at 200 rpm at 30 °C for 120 min. Afterward, the samples were filtered and the concentration of the dye remaining in the solution was determined by spectrophotometry (Pro-Análise, V-1200), at the

respective wavelengths of each dye (DR28 – 498 nm; AC27 – 520 nm; RR194 – 539 nm; DiR343 – 584 nm). The adsorption capacity was determined from Eq. 1 while the percentage of dye removal in Eq. 2.

$$q_e = \frac{(C_0 - C_e)V}{m} \quad (1)$$

$$R = \frac{(C_0 - C_e)}{C_0} 100 \quad (2)$$

where q_e (mg g^{-1}) represents the adsorption capacity at equilibrium, C_0 and C_e (mg L^{-1}) are the initial and equilibrium concentrations of the dyes, respectively; V (L) indicates the volume of the solution and m (g) the mass of adsorbent used; R (%) is the dye removal.

3.2.4 Evaluation of azo dye adsorption

To evaluate the best operating conditions for the adsorption system, the effect of granulometry with upper cut size (180, 425, and 850 μm), adsorbent dosage (1.25, 2.5, 5, and 10 g L^{-1}), and pH (5, 7, 9, 11) were studied. The tests were carried out in a batch system (200 rpm, 30 °C) using 200 mg L^{-1} of DR28 (100 mL) and 5 g L^{-1} of GPAT. All adsorption assays were performed in triplicate, with 95% confidence.

The kinetic study was performed at four dye concentrations (150, 220, 560, and 710 mg L^{-1}) of DR28 and 5 g L^{-1} of GPAT. The system was constantly agitated at 200 rpm and maintained at 30 °C until equilibrium. The adsorption assays were performed in triplicate, with 95% confidence.

Adsorption isotherms were performed by placing 5 g L^{-1} of GPAT in contact with a wide concentration range of DR28 dye solution (100-1260 mg L^{-1}) with an initial $\text{pH} \approx 7$, and the 100 mL reactor was constantly stirred at 200 rpm for 120 min under different temperatures (20, 30, 40, 50 °C). The adsorption assays were performed in triplicate, with 95% confidence.

To describe the kinetic behavior and obtain the adsorption parameters, the nonlinear models of pseudo-first order (Eq. 3), pseudo-second order (Eq. 4), and Elovich (Eq. 5) were used. The adsorption isotherms were adjusted by the models of Langmuir (Eq. 6), Freundlich (Eq. 7), and Sips (Eq. 8), while the thermodynamic study was performed by Gibbs free energy (Eq. 9), entropy (Eq. 10) and enthalpy (Eq. 10).

$$q_t = q_e(1 - \exp(-k_1 t)) \quad (3)$$

$$q_t = \frac{q_e^2 k_2 t}{1 + q_e k_2 t} \quad (4)$$

$$q_t = \frac{1}{\beta} + \ln(\alpha \beta t) \quad (5)$$

$$q_e = \frac{q_m K_L C_e}{1 + K_L C_e} \quad (6)$$

$$q_e = K_F C_e^{1/n_F} \quad (7)$$

$$q_e = \frac{q_m K_S C_e^{1/ns}}{1 + K_S C_e^{1/ns}} \quad (8)$$

$$\Delta G^0 = -RT \ln(K^0) \quad (9)$$

$$\ln(K^0) = \frac{\Delta S^0}{R} - \frac{\Delta H^0}{RT} \quad (10)$$

where, q_t (mg g^{-1}) is the adsorption capacity in time; t (min) represents the time; k_1 (min^{-1}) and k_2 ($\text{g mg}^{-1} \text{min}^{-1}$) are constants rate for PFO and PSO, respectively; k_{id} ($\text{mg g}^{-1} \text{min}^{-0.5}$) represents the intraparticle diffusion constant; C (mg g^{-1}) are constantly connected to the boundary layer; α ($\text{mg g}^{-1} \text{min}^{-1}$) initial rate adsorption; β (g mg^{-1}) related to the activation energy and surface coverage; q_m (mg g^{-1}) is the maximum adsorption capacity; K_L (L mg^{-1}) is the Langmuir constant; K_F ($\text{mg g}^{-1}(\text{mg L}^{-1})^{-1/n}$) is the Freundlich equilibrium constant; n_F is the Freundlich exponent; K_S ($\text{mg L}^{-1})^{-1/n}$ is the Sips equilibrium constant; ns is the Sips exponent. ΔG^0 (kJ mol^{-1}) is the Gibbs free energy; ΔS^0 ($\text{kJ mol}^{-1} \text{K}^{-1}$) and ΔH^0 ($\text{kJ mol}^{-1} \text{K}^{-1}$) represents entropy and enthalpy, respectively; K^0 is the thermodynamic equilibrium constant; R ($8.31 \times 10^{-3} \text{kJ mol}^{-1} \text{K}^{-1}$) is the Universal gas constant and T (K) is the temperature.

3.2.5 Geopolymer regeneration

The regeneration of the adsorbent was carried out by heat treatment. In this case, 5 g L^{-1} of virgin GPAT was placed in contact with a DR 28 dye solution of 400 mg L^{-1} to saturate the material, the system was constantly stirred at 200 rpm for 120 min at $30 \text{ }^\circ\text{C}$. After filtration and determination of the remaining dye concentration in the solution, the adsorbent (GPAT-A) was dried in an oven ($50 \text{ }^\circ\text{C}$ for 5 h) and regenerated by a new heat treatment at $500 \text{ }^\circ\text{C}$ for 120 min, receiving the name of GPAT-R. This process was repeated for 5 cycles of adsorption using the same sample

of regenerated adsorbent. The adsorption assays were performed in triplicate, with 95% confidence.

3.2.6 Selectivity of adsorbent

Aiming at greater applicability of the geopolymeric adsorbent, the dyes AR27, DR28, RR194, and DiR343 (Fig. 9) were used to evaluate the adsorbent selectivity. Thus, 5 g L⁻¹ of GPAT was placed in contact with 200 mg L⁻¹ dye solutions in a stirred batch system at 200 rpm for 120 min at 30 °C. The selectivity of the dyes was evaluated over a wide pH range (3, 5, 7, 9, and 11). The selectivity of the adsorbent was evaluated in relation to the percentage of color removed and the adsorption capacity (q_e). All adsorption assays were performed in triplicate, with 95% confidence.

3.2.7 Raw materials and geopolymer characterization

The chemical composition was determined by Fourier transform infrared spectroscopy (FTIR - Agilent Technologies, Cary 660), while the mineralogical composition was obtained by X-ray diffractometry (XRD - Rigaku MiniFlex600). The microstructure was investigated by morphological analysis using a scanning electron microscope (SEM - JOEL JSM-6390LV) equipped with energy dispersion spectroscopy (EDS), and the microstructure of the pores (BET/BJH) by adsorption/desorption of N₂ at 77K using an automatic analysis.

3.3 RESULTS AND DISCUSSION

3.3.1 Preliminary tests to design the research

To start the research, an analysis to optimize the formulation necessary for the geopolymerization of the aluminosilicate was carried out. According to Table 6 it can be seen that it was possible to reduce 4.7 g of Na₂SiO₃, adding water, forming the geopolymer with a solid structure with 2.74 molar ratio. At the molar ratio 2.07 and 2.41, it was observed that the material in contact with water dissolved, indicating that geopolymerization did not occur. Although the color removal results under these

conditions were superior, due to dissolution, a centrifugation process was required to separate the adsorbent from the liquid medium. In addition, the use of a powder adsorbent would be an obstacle to the use of columns of adsorption. So, as the objective is to structure an adsorbent GP, the second formulation with a molar ratio of 2.87 SiO₂/Al₂O₃ proved to be more suitable for the adsorption of the DR28 dye, as well as, it allows to reduce the use of sodium silicate. The GP with 2.87 molar ratio obtained $q_e = 7 \text{ mg g}^{-1}$ and $R = 12\%$.

Table 6 - Analysis of different formulations of alkaline activators for geopolymerization (Adsorption conditions: AD = 5 g L⁻¹, [DR28] = 15 mg L⁻¹, T = 30°C, A = 200 rpm, CT = 120 min, pH_i ≈ 7).

| MK/NaOH/Na ₂ SiO ₃ /H ₂ O | SiO ₂ /Al ₂ O ₃ molar ratio | GP formed? | W/S ^a | pH(f) | R (%) ^b | q _e (mg g ⁻¹) ^b |
|--|---|---------------|------------------|-------|--------------------|--|
| 20/6/14.71/0 | 3.06 | Yes | 0.46 | 10.22 | 17.16 | 9.82 |
| 20/6/12/1 | 2.87 | Yes | 0.46 | 10.02 | 12.31 | 7.05 |
| 20/6/10/1.7 | 2.74 | Yes | 0.46 | 9.62 | 7.09 | 4.06 |
| 20/6/5/5.8 | 2.41 | No | 0.56 | 8.69 | 35.07 | 20.07 |
| 20/6/0/13 | 2.07 | No | 0.83 | 8.15 | 72.39 | 41.43 |

Note: AD – Adsorbent Dosage; [DR28] – Concentration of dye; T – Temperature; A – Agitation; CT – Contact Time.

^a Water/solid proportion in weight

^b Adsorption of DR28

Furthermore, as the literature has shown, acid etching can improve the adsorptive properties, increasing the surface area (Chen et al., 2022). However, the effects of calcination of geopolymers were not clear. Thus, in a preliminary way, it was sought to understand whether the temperature would have any effect on the adsorption of DR28, as well as to choose between phosphoric and sulfuric acid which one to use. According to preliminary tests (Table 7) H₂SO₄ promotes modifications capable of improving DR28 removal when compared to H₃PO₄, for this reason, it was used in subsequent tests, as well as it was verified that there was an improvement in the removal of the dye DR28 with calcination.

Table 7 - Preliminary evaluation of acid attack (sulfuric acid and phosphoric acid) and calcination conditions for geopolymer modification (Adsorption conditions: AD = 5 g L⁻¹, [DR28] = 15 mg L⁻¹, T = 30°C, A = 200 rpm, CT = 120 min, pH_i ≈ 7).

| Attack acid | Calcination (°C) | R (%) ^a | q _e (mg g ⁻¹) ^a |
|--------------------------------|------------------|--------------------|---|
| H ₂ SO ₄ | 500 | 93.64 | 2.08 |
| H ₂ SO ₄ | No | 30.25 | 0.67 |
| H ₃ PO ₄ | 500 | 65.70 | 1.46 |
| H ₃ PO ₄ | No | 12.14 | 0.27 |

Note: AD – Adsorbent Dosage; [DR28] – Concentration of dye; T – Temperature; A – Agitation; CT – Contact Time.

^a Adsorption of DR28

3.3.2 Influence GP modification

The influence of H₂SO₄ concentration and calcination temperature used to modify the GP was investigated by a CCRD design, achieving optimization of the conditions for the development of a highly efficient adsorbent. As seen in Table 8, only the acid concentration positively affects the two responses ($q_e = 27.04$ (mg g⁻¹); $R = 65.25$), therefore, the increase in the concentration of H₂SO₄ indicates a greater capacity for adsorption and removal of the dye. The calcination temperature within the investigated limits was insignificant ($p > 0.05$) which allows the use of milder temperatures to produce the geopolymer, reducing energy costs.

Table 8 - Estimated effects, errors, and p -values of the adsorption capacity and dye removal on modified GP.

| Factor | Response | | | | | |
|--|--------------------------|------------|-------------------------|--------|------------|-------------------------|
| | qe (mg g ⁻¹) | | | R (%) | | |
| | Effect | Pure error | p -value ^a | Effect | Pure error | p -value ^a |
| Mean | 40.78 | 2.12 | <0.0001 | 98.40 | 5.11 | <0.0001 |
| H ₂ SO ₄ (L) | 27.04 | 2.59 | 0.0001 | 65.25 | 6.26 | 0.0001 |
| H ₂ SO ₄ (Q) | -22.06 | 3.09 | 0.0008 | -53.22 | 7.45 | 0.0008 |
| Calcination (L) | 3.99 | 2.59 | 0.1846 | 9.46 | 6.26 | 0.1846 |
| Calcination (Q) | -1.73 | 3.09 | 0.5994 | -4.17 | 7.46 | 0.5995 |
| H ₂ SO ₄ x Calcination | -4.41 | 3.67 | 0.2829 | -10.66 | 8.86 | 0.2829 |

^a Confidence interval of 95%. L = linear effect; Q = quadratic effect.

Two quadratic models were proposed to describe the experimental data and predict the best adsorbent production conditions. The models referring to adsorption capacity (Eq. 11) and dye removal (Eq. 12) were validated by analysis of variance (Table 9), with correlation coefficients $R^2 > 0.97$.

Table 9 - Analysis of variance of the CCRD on the adsorption and removal capacity of the dye.

| Variation source | SS | DF | MS | F _{cac} | F _{tab} |
|---------------------|----------|----|----------|------------------|------------------|
| Qe | | | | | |
| Regression | 2207.85 | 5 | 207.85 | 33.15 | 5.05 |
| Residual | 67.53 | 5 | 13.51 | | |
| Total | 2275.38 | 10 | | | |
| R ² 0.97 | | | | | |
| R | | | | | |
| Regression | 12852.02 | 5 | 12852.02 | 33.15 | 5.05 |
| Residual | 393.07 | 5 | 393.07 | | |
| Total | 13425.09 | 10 | | | |
| R ² 0.97 | | | | | |

Note: SS – Sum of square; DF – Degrees of freedom; MS – Mean squared

In addition, Fischer's F test was used to validate the results. For Eqs. 11 and 12, the calculated F value (F_{calc}) was 33.15 while the default F value (F_{std}) was 5.05, demonstrating the predictive power of the model ($F_{calc} > F_{std}$).

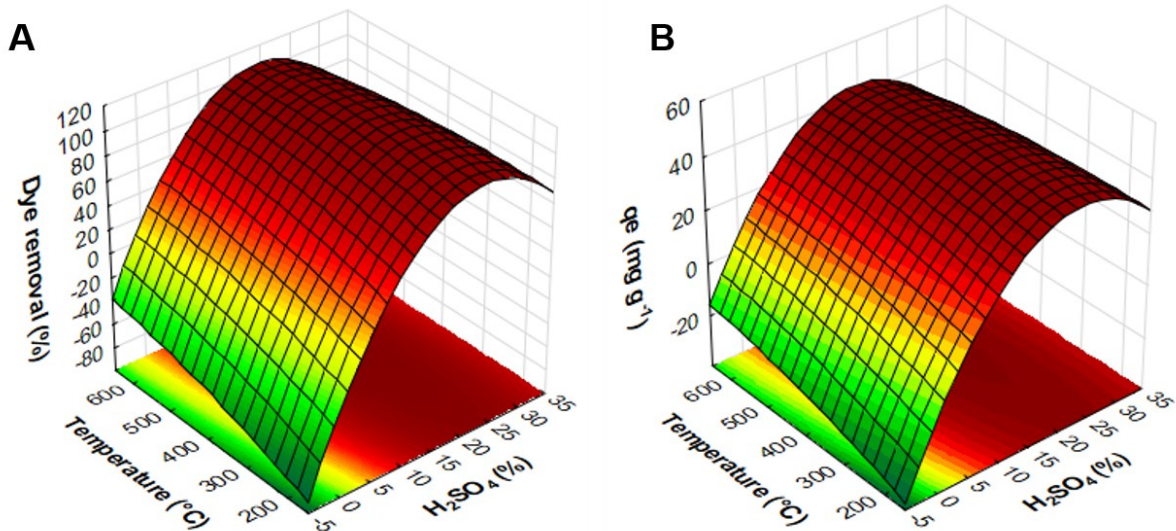
$$qe \text{ (mg g}^{-1}\text{)} = -21.86 + 4.81x_1 - 0.98x_1^2 + 0.71x_2 \quad (11)$$

$$R \text{ (\%)} = -52.75 + 11.60x_1 - 0.23x_1^2 + 0.17x_2 \quad (12)$$

where x_1 and x_2 are the coded values of H_2SO_4 concentration and temperature of calcination, respectively.

Since the models are valid and significant, then it becomes possible to generate the response surfaces for the results as a function of the adsorption capacity (qe) and dye removal (R), as shows Fig. 10. In Fig. 10a, it is verified that the best conditions (higher qe) are found when the concentration of H_2SO_4 is greater than 15%, regardless of the calcination temperature. Similar results are found for dye removal (Fig. 10b), where percentages above 95% are found when 15% acid is used at any calcination temperature. These results agree with the study of the effect of variables, which showed that only the concentration of H_2SO_4 influences the responses. It should be noted that temperature can contribute to the modification of GP, although it was not significant within the range evaluated in the CCRD. Preliminary results (Table 7) indicated that the thermal treatment increases the adsorption of DR28 when compared to the GP only modified with acid.

Fig. 10 - Response surface as a function of (a) dye removal and (b) the adsorption capacity of the modified GP (Adsorption conditions: AD = 5 g L⁻¹, [DR28] = 200 mg L⁻¹, T = 30°C, A = 200 rpm, CT = 120 min, pH_i ≈ 7).



Note: AD – Adsorbent Dosage; [DR28] – Concentration of dye; T – Temperature; A – Agitation; CT – Contact Time.

Source: the author

When checking the matrix tests (Table 10), it is noticed that in experiment n. 5, H₂SO₄ was not used, consequently, the adsorption of DR28 did not occur, corroborating the previously described result. However, condition 7 of the planning shows good results, with $q_e = 40.85 \text{ mg g}^{-1}$ and dye removal near 98.53%. Thus, the GP was placed in contact with 15% of H₂SO₄ and calcined for 120 min at 200 °C for modification and production of the adsorbent. The GP modified only with acid was named GPA and the one that suffered acid and thermal treatment was named GPAT.

Table 10 - Experimental planning of GP production (real values) and responses regarding adsorption capacity and dye removal, and preliminary evaluation of pH effect (Adsorption conditions: AD = 5 g L⁻¹, [DR28] = 200 mg L⁻¹, T = 30°C, A = 200 rpm, CT = 120 min, pH_i ≈ 7).

| Assay | Variables | | Response | | pH analysis | | |
|-------|------------------------------------|------------------|--------------------------------------|-------|-------------------------------|------------------------------|------------------------------|
| | H ₂ SO ₄ (%) | Temperature (°C) | q _e (mg g ⁻¹) | R (%) | pH _{GP} ^a | pH _i ^b | pH _f ^c |
| 1 | 4.4 | 258.6 | 8.39 | 20.25 | 6.16 | 7.03 | 6.30 |
| 2 | 25.6 | 258.6 | 37.75 | 91.07 | 5.17 | 7.00 | 5.58 |
| 3 | 4.4 | 541.4 | 20.60 | 49.69 | 6.20 | 6.98 | 6.28 |
| 4 | 25.6 | 541.4 | 41.11 | 99.19 | 4.88 | 7.01 | 3.98 |
| 5 | 0 | 400 | 0 | 0 | 6.85 | 7.05 | 6.45 |
| 6 | 30 | 400 | 41.25 | 99.53 | 4.34 | 7.03 | 3.78 |
| 7 | 15 | 200 | 40.84 | 98.53 | 5.47 | 7.00 | 4.44 |
| 8 | 15 | 600 | 41.13 | 99.24 | 4.83 | 6.95 | 4.18 |
| 9 | 15 | 400 | 40.82 | 98.48 | 5.47 | 7.04 | 5.27 |
| 10 | 15 | 400 | 40.52 | 97.77 | 5.80 | 6.94 | 4.78 |
| 11 | 15 | 400 | 41.03 | 98.99 | 5.72 | 6.98 | 4.43 |

Note: AD – Adsorbent Dosage; [DR28] – Concentration of dye; T – Temperature; A – Agitation; CT – Contact Time.

^a GP pH measured in water after washing

^b Initial pH of the DR28 solution

^c Final pH after DR28 adsorption

From the monitoring of the pH values for each trial of the experimental design (Table 10), it is possible to verify that there were pH changes before and after the adsorption. The aqueous solutions of dye-containing dyes were prepared with distilled water, so the pH_i (before adsorption) was around 7. However, after placing the adsorbent in contact with the aqueous solution and remaining there during the 120 min of reaction, it was observed that pH decay at the end of the adsorption (pH_f). This pH change is directly linked to the pH of the geopolymer (pH_{GP}) which was determined after successive washing cycles of the GP with water. As previously mentioned, washing was carried out until the pH variation was no longer observed. It is observed that the lowest pH values are for samples that had contact with high concentrations of H₂SO₄ (>15%). As verified in the EDS analysis (Fig. 19), the presence of sulfur was

identified in the samples, indicating that this element impregnated the GP, not being removed with the washing. However, as the adsorption results were efficient in terms of color removal and adsorptive capacity, it was decided not to buffer the solution.

3.3.3 Evaluation of azo dye adsorption

Once the GPAT preparation conditions were defined, the influence of the particle size on the adsorption was evaluated (180, 425, and 850 μm), as shown in Table 11. It is known that the smaller the particle size the larger the specific surface area. However, there was no significant difference between GPAT sizes in the adsorption efficiency of DR28. Thus, due to the ease of separation, expansion of column scale, and reuse of the adsorbent, we standardized the size at $<425 \mu\text{m}$.

The dosage of the adsorbent is an important condition to avoid the excessive use of GPAT. In Table 11, it is observed that in dosages above 5 g L^{-1} the removal of DR28 reaches $\sim 99\%$, but the q_e decreases from ~ 57 to $\sim 23 \text{ mg g}^{-1}$ with overdose. According to Eq. 1, the mass of the adsorbent is inversely proportional to the adsorption capacity, therefore, increasing the dosage causes a drop in q_e . Thus, to ensure good q_e and R , it was decided to follow the tests with 5 g L^{-1} .

The decision not to adjust the pH of the dye solution for the tests was based on the results found in Table 11. In alkaline pH (11) a reduction of q_e ($\sim 27 \text{ mg g}^{-1}$) and R (67%) was observed, while in the range of pH 5-9, the results were maintained with $q_e \sim 39 \text{ mg g}^{-1}$ and $R \sim 99\%$. Thus, it was decided not to adjust the pH for the tests.

Table 11 - Effect of particle size, adsorbent dosage, and pH value on DR28 adsorption (Adsorption conditions: AD = 5 g L⁻¹, [DR28] = 200 mg L⁻¹, T = 30°C, A = 200 rpm, pH ≈ 7).

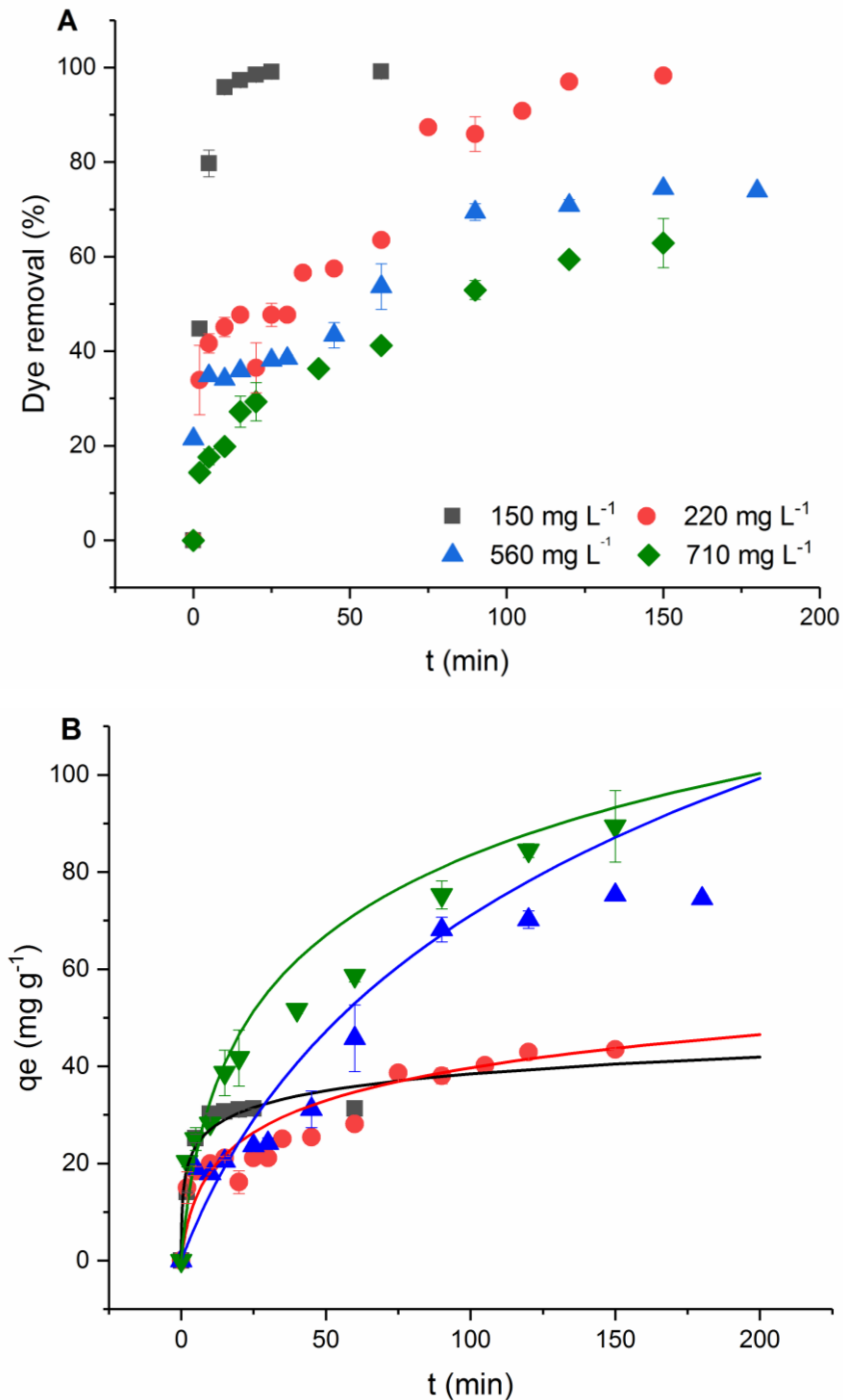
| | q_e (mg g ⁻¹) | R (%) |
|------------------------------------|-----------------------------|--------------|
| Particle size (μm) | | |
| 180 | 39.64 ± 0.09 | 98.67 ± 0.23 |
| 425 | 39.78 ± 0.05 | 99.03 ± 0.12 |
| 850 | 39.30 ± 0.03 | 97.82 ± 0.07 |
| Adsorbent dosage (g/L) | | |
| 1.25 | 57.47 ± 3.59 | 30.71 ± 1.92 |
| 2.50 | 51.11 ± 4.67 | 54.62 ± 4.99 |
| 5.00 | 46.37 ± 0.01 | 99.11 ± 0.03 |
| 10.00 | 23.24 ± 0.01 | 99.35 ± 0.06 |
| Initial pH of the solution* | | |
| 5 | 39.85 ± 0.17 | 99.19 ± 0.43 |
| 7 | 39.90 ± 0.05 | 99.30 ± 0.12 |
| 9 | 39.91 ± 0.02 | 99.33 ± 0.05 |
| 11 | 26.95 ± 0.36 | 67.09 ± 0.89 |

Note: AD – Adsorbent Dosage; [DR28] – Concentration of dye; T – Temperature; A – Agitation; CT – Contact Time.

*After adsorption the pH values ranged from 4.21 to 5.21

The kinetic study was performed with high dye concentrations (150-710 mg L⁻¹), as shown in Fig. 11a, with the best conditions of other parameters (5 g L⁻¹ of adsorbent at pH 7). For the lowest concentration, in 10 min the removal of DR28 was ~95%, demonstrating the high affinity between GPAT and the dye. For the other concentrations, equilibrium was reached in about 150 min. At equilibrium, it was observed that at the lowest 150 and 220 mg L⁻¹ the dye was adsorbed with high efficiency (R > 98%), however with increasing concentration there was saturation of GPAT and the efficiency drops to 74% (560 mg L⁻¹) and 62% (710 mg L⁻¹). However, for application as an adsorbent, these results are very satisfactory, since adsorption is an advanced process, used as a polish, after conventional processes. In Fig. 11b, an increase in q_e can be seen at higher concentrations. For example, with 150 mg L⁻¹ of DR28 the GPAT obtained $q_e = 31.26$ mg g⁻¹, with 710 mg L⁻¹ the $q_e = 89.38$ mg g⁻¹.

Fig. 11 - (A) DR28 removal kinetics and (B) adjustments of Elovich kinetic adsorption model to experimental data (Adsorption conditions: AD = 5 g L⁻¹, [DR28] = 150-710 mg L⁻¹, T = 30°C, A = 200 rpm, pH ≈ 7).



Note: AD – Adsorbent Dosage; [DR28] – Concentration of dye; T – Temperature; A – Agitation; CT – Contact Time.

Source: the author

The kinetic mass transfer mechanisms that control the adsorption of DR28 on GPAT were investigated and are fully described in Table 12. The high values of

correlation coefficients and lower error values indicate that the Elovich model adequately represents the experimental data. Elovich satisfactorily describes heterogeneous processes, where the adsorbate is deposited on the surface of the adsorbent attracted by chemical bonds (Wang and Guo, 2020). Thus, it can be assumed that chemisorption has a strong influence on the adsorption of DR28 on GPAT. Table 12 shows the Elovich parameters, in which it is observed that α and β decrease with increasing concentration. In processes where an external mass transfer is controlled by external diffusion, the concentration gradient has a strong influence. However, for the adsorption of DR28 on GPAT under conditions with a lower concentration, the adsorption rate is higher ($109.10 \text{ mg g}^{-1} \text{ min}^{-1}$). This reinforces the hypothesis that the controlling mechanism is of chemical and not physical origin.

Table 12 - Kinetic parameters for DR28 adsorption onto GPAT (Adsorption conditions: AD = 5 g L^{-1} , [DR28] = $150\text{-}710 \text{ mg L}^{-1}$, T = 30°C , A = 200 rpm, pH ≈ 7).

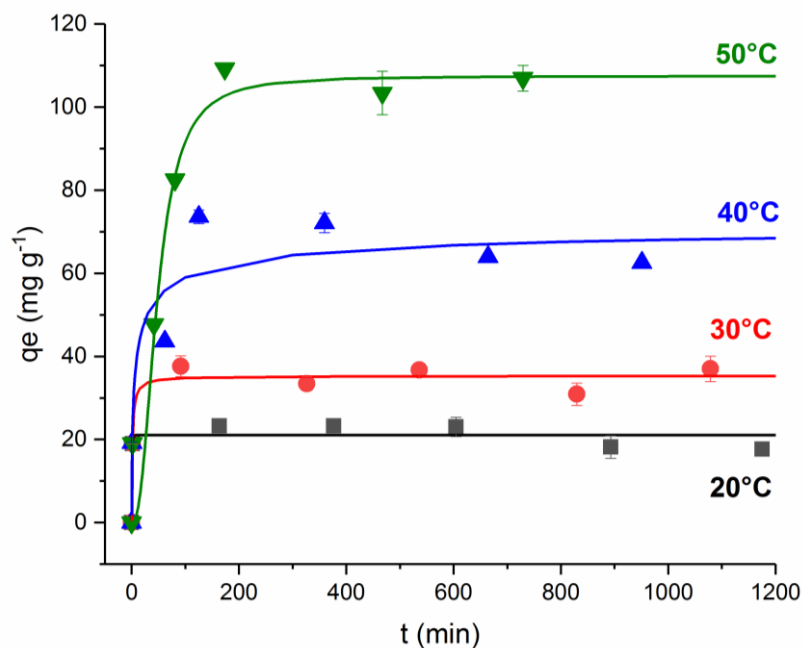
| Kinetic model | Concentrations | | | |
|--|--------------------------------|---|---|---|
| | 150 mg L^{-1} | 220 mg L^{-1} | 560 mg L^{-1} | 710 mg L^{-1} |
| $q_{E,exp} \text{ (mg g}^{-1}\text{)}$ | 31.26 | 43.50 | 75.27 | 89.38 |
| Pseudo-first order (PFO) | | | | |
| $q_1 \text{ (mg g}^{-1}\text{)}$ | 31.24 ± 0.09 | 41.08 ± 1.55 | 84.62 ± 6.76 | 81.60 ± 1.41 |
| $k_1 \text{ (min}^{-1}\text{)}$ | 0.31 ± 0.01 | $0.03 \pm 3.70 \times 10^{-3}$ | $0.01 \pm 2.90 \times 10^{-3}$ | $0.03 \pm 1.54 \times 10^{-3}$ |
| R^2 | 0.9994 | 0.7458 | 0.9461 | 0.9046 |
| R^2_{adj} | 0.9993 | 0.7277 | 0.9307 | 0.8940 |
| HYBRID | 27.47 | 10.18 | 10.73 | 9.71 |
| SSE | 13.10 | 5.86 | 9.26 | 8.57 |
| Pseudo-second order (PSO) | | | | |
| $q_2 \text{ (mg g}^{-1}\text{)}$ | 34.37 ± 0.04 | 47.73 ± 4.02 | 118.10 ± 15.00 | 97.00 ± 1.59 |
| $k_2 \text{ (g mg}^{-1} \text{ min}^{-1}\text{)}$ | $0.01 \pm 0.50 \times 10^3$ | $0.08 \times 10^{-3} \pm 0.04 \times 10^{-3}$ | $0.01 \times 10^{-3} \pm 0.06 \times 10^{-3}$ | $4.08 \times 10^{-4} \pm 0.01 \times 10^{-3}$ |
| R^2 | 0.9835 | 0.7941 | 0.9447 | 0.9403 |
| R^2_{adj} | 0.9807 | 0.7794 | 0.9391 | 0.9336 |
| HYBRID | 21.84 | 8.24 | 6.29 | 5.73 |
| SSE | 11.52 | 5.29 | 6.06 | 6.60 |
| Elovich | | | | |
| $\alpha \text{ (mg g}^{-1} \text{ min}^{-1}\text{)}$ | 109.10 ± 13.29 | 5.19 ± 3.43 | 1.57 ± 0.35 | 6.79 ± 0.31 |
| $\beta \text{ (g mg}^{-1}\text{)}$ | $0.20 \pm 3.50 \times 10^{-3}$ | 0.10 ± 0.02 | $0.02 \pm 5.30 \times 10^{-3}$ | $0.04 \pm 8.80 \times 10^{-4}$ |
| R^2 | 0.9330 | 0.8614 | 0.9442 | 0.9697 |
| R^2_{adj} | 0.9219 | 0.8515 | 0.9386 | 0.9664 |
| HYBRID | 11.45 | 4.98 | 5.50 | 8.19 |
| SSE | 8.57 | 4.33 | 5.97 | 5.48 |

Note: AD – Adsorbent Dosage; [DR28] – Concentration of dye; T – Temperature; A – Agitation; CT – Contact Time.

The adsorption isotherms of DR28 in GPAT are shown in Fig. 12. The curves very close to the y-axis indicate a favorable process (Ruthven, 1984), yet the increase in temperature is responsible for higher values of adsorption capacity, at 293 K the $q_e \sim 20 \text{ mg g}^{-1}$, while in 323K the $q_e \sim 100 \text{ mg g}^{-1}$, suggesting an endothermic process. In

addition, the increase in temperature decreases the viscosity of the fluid and increases the mobility of the adsorbate, as a consequence the rates of diffusion of DR28 molecules through the boundary layer increase (Tochetto et al., 2022a). Considering that textile dyeing processes generally take place in a heated bath, the fact that the effluent is at high temperatures is an advantage for the process, not requiring cooling to ensure the good performance of the adsorbent. This behavior may be linked to GPAT swelling, exposing more sites available for sorption. To exemplify this effect, at the lowest dye concentration (100 mg L^{-1}), at all temperatures, from 20 to $50 \text{ }^{\circ}\text{C}$, DR28 was completely adsorbed ($R > 99\%$). However, the effect of temperature can be clearly visualized with the highest concentration used in the isotherms. When GPAT was placed in contact with 1200 mg L^{-1} , it was observed that at $20 \text{ }^{\circ}\text{C}$ the $R \sim 7\%$, at $30 \text{ }^{\circ}\text{C}$ the $R \sim 15\%$, at $40 \text{ }^{\circ}\text{C}$ the $R \sim 25\%$ and at $50 \text{ }^{\circ}\text{C}$ removal was $\sim 43\%$. These results are very interesting, mainly because, as mentioned, the textile effluent arrives in the treatment at higher temperatures and these removal data demonstrate the advantage of the adsorbent.

Fig. 12 - Isotherm adsorption curves for DR28 on GPAT fitted to the Sips model (Adsorption conditions: $AD = 5 \text{ g L}^{-1}$, $[DR28] = 100\text{-}1200 \text{ mg L}^{-1}$, $T = 20\text{-}50^{\circ}\text{C}$, $A = 200 \text{ rpm}$, $CT = 120 \text{ min}$, $\text{pH} \approx 7$).



Note: AD – Adsorbent Dosage; $[DR28]$ – Concentration of dye; T – Temperature; A – Agitation; CT – Contact Time.

Source: the author

Table 13 - Isotherm parameters for DR28 adsorption onto GPAT (Adsorption conditions: AD = 5 g L⁻¹, [DR28] = 100-1200 mg L⁻¹, T = 20-50°C, A = 200 rpm, CT = 120 min, pH ≈ 7).

| Isotherm model | Temperature | | | |
|---|---|--------------|--------------|---|
| | 293 K | 303 K | 313 K | 323 K |
| $q_{e,exp}$ (mg g ⁻¹) | 23.27 | 37.63 | 73.61 | 109.21 |
| Langmuir | | | | |
| q_m (mg g ⁻¹) | 21.08 ± 0.08 | 35.30 ± 0.68 | 64.17 ± 0.05 | 117.50 ± 4.00 |
| K_L (L g ⁻¹) | 5.60 ± 0.83 | 0.71 ± 0.10 | 0.45 ± 0.12 | 0.02 ± 3.64x10 ⁻³ |
| R^2 | 0.9175 | 0.9692 | 0.8924 | 0.9479 |
| R^2_{adj} | 0.9010 | 0.9631 | 0.8709 | 0.9374 |
| HYBRID | 1.25 | 0.46 | 3.17 | 11.06 |
| SSE | 2.19 | 2.25 | 8.64 | 10.22 |
| Freundlich | | | | |
| K_F (mg g ⁻¹ (mg L ⁻¹) ^{-1/n}) | 20.29 ± 0.41 | 21.65 ± 0.93 | 28.44 ± 0.12 | 27.33 ± 1.06 |
| n_F | 4.10x10 ⁻³ ± 4.32x10 ⁻³ | 13.08 ± 0.82 | 7.35 ± 0.08 | 4.52 ± 0.21 |
| R^2 | 0.9094 | 0.9190 | 0.8646 | 0.9094 |
| R^2_{adj} | 0.8913 | 0.9028 | 0.8375 | 0.8912 |
| HYBRID | 1.32 | 1.45 | 4.66 | 6.12 |
| SSE | 2.29 | 3.65 | 9.69 | 12.52 |
| Sips | | | | |
| q_m (mg g ⁻¹) | 21.08 ± 0.08 | 35.14 ± 0.66 | 72.60 ± 9.59 | 107.50 ± 2.10 |
| K_S (mg L ⁻¹) ^{-1/n} | 2.35 ± 1.63 | 0.16 ± 0.15 | 0.36 ± 0.18 | 1.08x10 ⁻⁴ ± 1.37x10 ⁻⁴ |
| n_s | 0.37 ± 0.14 | 0.26 ± 0.05 | 1.85 ± 1.70 | 0.42 ± 0.03 |
| R^2 | 0.9178 | 0.9712 | 0.9140 | 0.9652 |
| R^2_{adj} | 0.9020 | 0.9669 | 0.8709 | 0.9477 |
| HYBRID | 1.25 | 0.43 | 1.96 | 14.34 |
| SSE | 2.18 | 2.18 | 7.73 | 7.76 |

Note: AD – Adsorbent Dosage; [DR28] – Concentration of dye; T – Temperature; A – Agitation; CT – Contact Time.

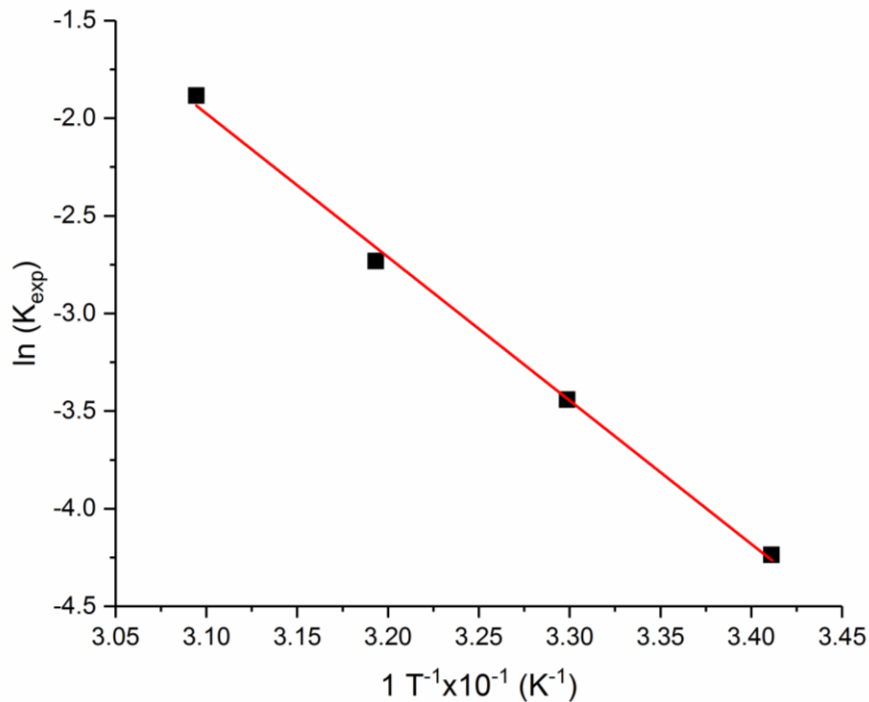
The parameters and adjustment coefficients of the models are described in Table 13. The Langmuir and Sips models obtained the best adjustments for this adsorptive process, however considering the correlation coefficients (R^2 and R^2_{adj}) and smaller error values (HYBRID and SSE), it is suggested that it was found that the Sips model was able to represent the data more accurately for the four temperatures. As observed in Table 13, the q_e values obtained experimentally are very close to those predicted by the models (q_m), confirming a good fit. Sips is an empirical model based on the combination of the Langmuir and Freundlich equations, applied to heterogeneous systems (Sips, 1948).

The maximum adsorption capacity as indicated by the Sips model is 107.50 mg g⁻¹, which makes GPAT highly competitive against other modified geopolymers for removing azo dyes. GP produced with H₂O₂ and magnetized showed $q_e = 41.8$ mg g⁻¹ for the adsorption of Procion Red (Hua et al., 2020). Acid activation with H₃PO₄

produced GPAC with $q_e = 39.1 \text{ mg g}^{-1}$ to remove Eriochrome Black T (Tome et al., 2021). A strategy similar to that used in this work was also investigated by Fumba et al. (2014), who, after synthesizing GP, performed calcination at $700 \text{ }^\circ\text{C}$. In that case, however, $q_e = 0.3 \text{ mg g}^{-1}$, did not affect the adsorption of Methyl Orange.

The thermodynamic study of the adsorption of DR28 on GPAT was performed with the van't Hoff plot (Fig. 13) and the effect of temperature was evaluated in the range of 293-323 K.

Fig. 13 - Van't Hoff plot obtained from the thermodynamic study at different temperatures of DR28 adsorption in GPAT (Adsorption conditions: AD = 5 g L^{-1} , [DR28] = $100\text{-}1200 \text{ mg L}^{-1}$, T = $20\text{-}50^\circ\text{C}$, A = 200 rpm, CT = 120 min, pH ≈ 7).



Note: AD – Adsorbent Dosage; [DR28] – Concentration of dye; T – Temperature; A – Agitation; CT – Contact Time.

Source: the author

In Table 14, it can be seen that the ΔG^0 value is negative, indicating that the adsorption of DR28 on GPAT is spontaneous. ΔG^0 decreases with increasing temperature, reinforcing the experimental results of isotherms, which showed an increase in adsorption capacity with increasing temperature. The negative value of the ΔH^0 indicates that the adsorption has an exothermic character and that the physical adsorption has influence on the process. The results of the isotherms indicated that the process has an endothermic characteristic. In general, one type exerts greater

influence, but it is possible to observe the occurrence of exothermic and endothermic processes simultaneously (Al-Ghouti et al., 2019). While the positive value of the ΔS^0 suggests the occurrence of rearrangements in the solid-liquid interface during the adsorption.

Table 14 - Thermodynamic parameters of DR28 adsorption on GPAT (Adsorption conditions: AD = 5 g L⁻¹, [DR28] = 100-1200 mg L⁻¹, T = 20-50°C, A = 200 rpm, CT = 120 min, pH ≈ 7).

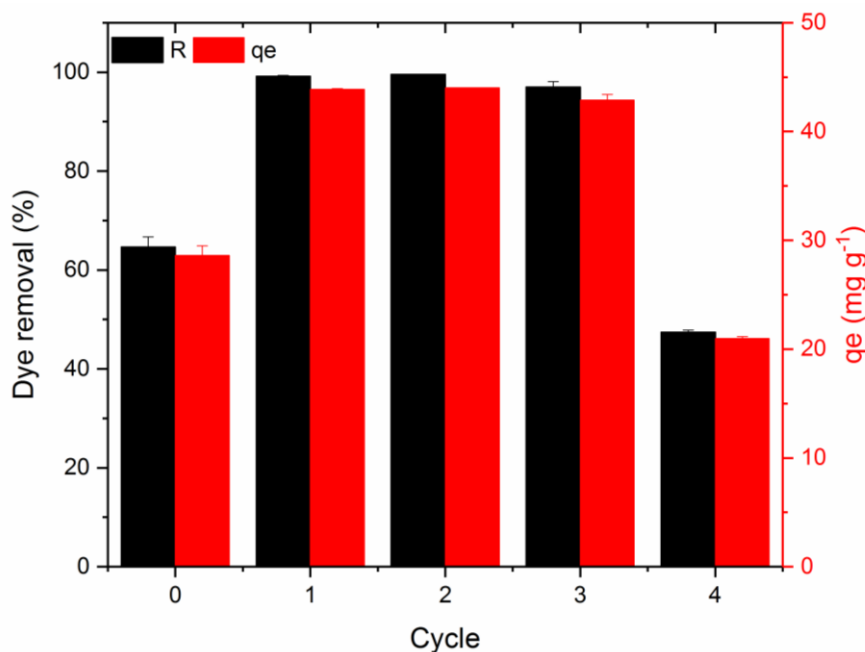
| T (K) | ΔS^0 (kJ mol ⁻¹ K ⁻¹) | ΔH^0 (kJ mol ⁻¹ K ⁻¹) | ΔG^0 (kJ mol ⁻¹) |
|-------|--|--|--------------------------------------|
| 293 | 0.17 ± 0.01 | -0.06 ± 3.06x10 ⁻³ | -52.83 ± 2.85 |
| 303 | | | -54.63 ± 2.94 |
| 313 | | | -56.43 ± 3.04 |
| 323 | | | -58.23 ± 3.14 |

Note: AD – Adsorbent Dosage; [DR28] – Concentration of dye; T – Temperature; A – Agitation; CT – Contact Time.

3.3.4 Regeneration of GPAT

Fig. 14 presents the GPAT regeneration results. It is possible to observe that q_e rises from 28.61 to 43.87 mg g⁻¹ after regeneration, representing an increase of ~35%. Regarding the specific area (Table 15), it was noticed that although there was an increase in q_e , there was a decrease in the specific area with regeneration. Thus, it can be assumed that chemical adsorption had a greater influence or even multilayer adsorption. Likewise, Novais et al. (2018) noticed that regeneration above 200 °C causes the removal of physically adsorbed water in the GP and, as a consequence, increases the number of active sites for adsorption. GPAT-R maintains the high q_e for 3 cycles, decreasing by half in the 4th cycle. Similar behavior is observed for the removal of DR28, after regeneration, the percentages were close to 100%.

Fig. 14 - Effect of GPAT regeneration on the adsorption capacity and removal efficiency of DR28 (Adsorption conditions: AD = 5 g L⁻¹, [DR28] = 400 mg L⁻¹, T = 30°C, A = 200 rpm, CT = 120 min, pH ≈ 7; Regeneration conditions: T = 500°C, CT = 120 min).



Note: AD – Adsorbent Dosage; [DR28] – Concentration of dye; T – Temperature; A – Agitation; CT – Contact Time.

Source: the author

3.3.5 GPAT selectivity and effect of pH for azo dye adsorption

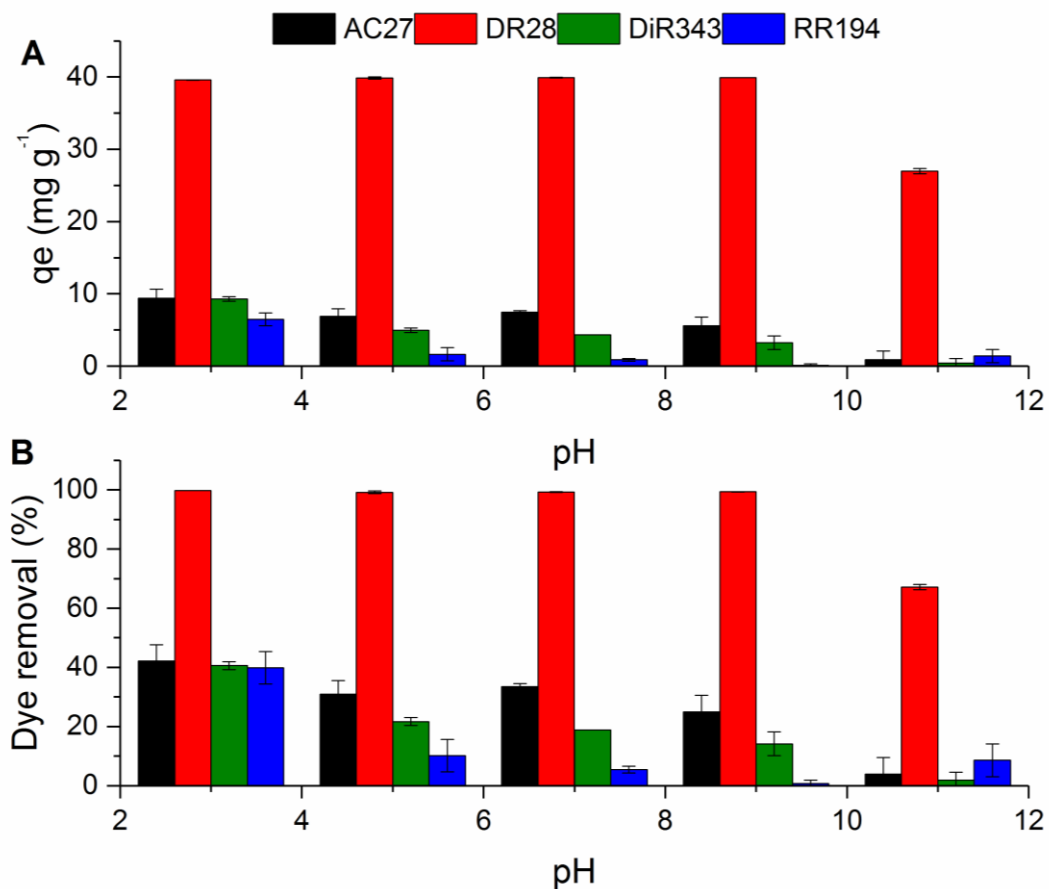
The selectivity of the adsorbent was evaluated under different azo dyes and different pH conditions because each dye solution has its own application condition in dyeing processes, that is pH and temperature. Fig. 15 shows that DR28 had the highest affinity with GPAT, followed by AC27, RR194, and DiR343. The highest removal efficiencies are at acidic pH, however, for DR28, it is observed that the values are close to 100% at pH 3 to 9. This result corroborates the previously described results that point to a control of the chemisorption in the process.

It was expected that dyes with the same electrical charge would have the same performance in the adsorption process because the attraction or repulsion of charges is a strong supporting in the dyeing process, which happens to be an adsorption process as well. However, this hypothesis was not confirmed. Therefore, we cannot

assume that dyes with the same electrical charge will have the same adsorption performance with the geopolymer studied.

To strengthen this discussion of the influence of electrical charges, the zeta potential of the dyes and the adsorbent should be measured. Unfortunately, the zeta potential experiments could not be performed for the adsorbent, as it did not withstand the pressure conditions of the test and was partially solubilized, making it unfeasible to carry out the test. The zeta potential of the dyes was also not performed due to the difficulty of finely adjusting the pH as required by the experiment. Therefore, the discussion regarding the influence of the electric charge and the isoelectric point of each dye and the geopolymer cannot be established.

Fig. 15 - Evaluation of selectivity of GPAT for adsorption of azo dyes in a wide range of pH (Adsorption conditions: AD = 5 g L⁻¹, [DR28] = 200 mg L⁻¹, T = 30°C, A = 200 rpm, CT = 120 min).



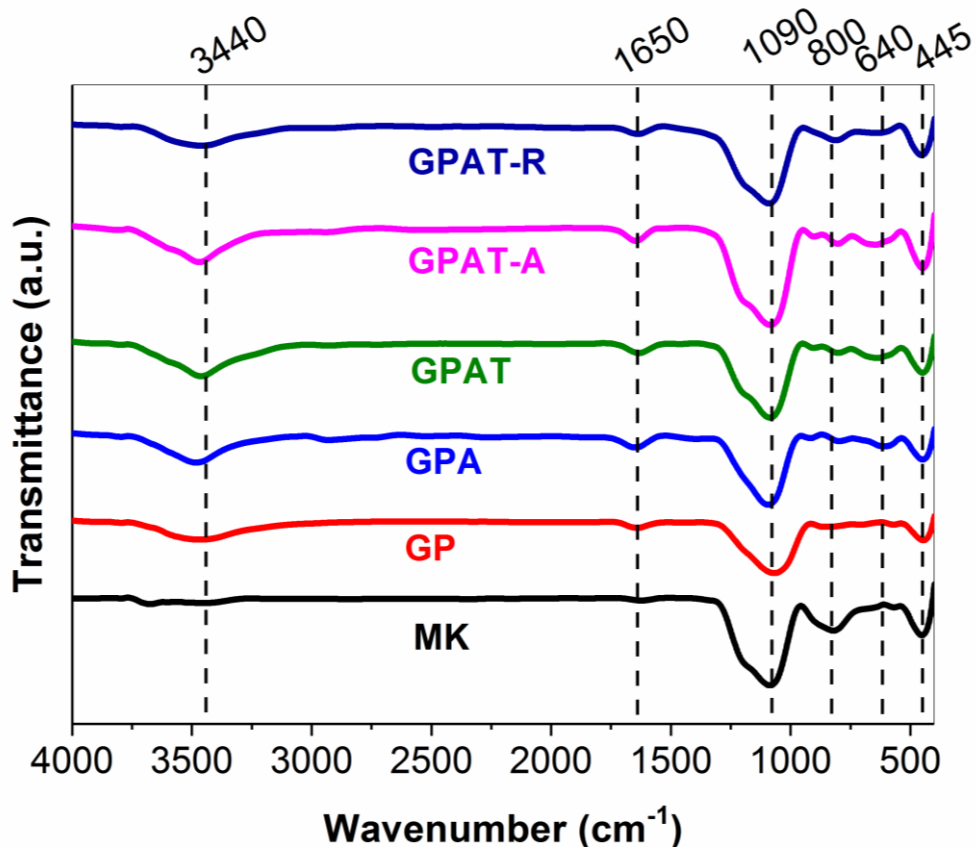
Note: AD – Adsorbent Dosage; [DR28] – Concentration of dye; T – Temperature; A – Agitation; CT – Contact Time.

Source: the author

3.3.6 Effect of changes in GP characteristics

FTIR results of geopolymer samples are depicted in Fig. 16. The peaks close to the region of 3440 cm^{-1} can be attributed to the O-H elongation of the silane groups and adsorbed water was observed in the geopolymer samples. In the MK it does not appear (Rossatto et al., 2020; Somna et al., 2011). The H-O-H vibration of water can also be found at 1650 cm^{-1} in all samples (Somna et al., 2011). According to Barbosa et al. (2018), the bands between 1100 and 1000 cm^{-1} correspond to asymmetric stretching vibrations of Si-O-T (T = Si or Al) in MK (1074 cm^{-1}), GP (1081 cm^{-1}), GPA (1093 cm^{-1}), GPAT (1083 cm^{-1}), GPAT-A (1083 cm^{-1}) and GPAT-R (1091 cm^{-1}). The subtle change in the position of the peaks in the 1090 cm^{-1} region of the MK compared to the GP samples indicates alkaline activation (NaOH) and, therefore, geopolymerization (Barbosa, 2018). The sharpest peak at 813 cm^{-1} of MK indicates the presence of Si-O-T symmetric elongation, while in geopolymerized samples this peak does not appear or is very subtle, because during geopolymerization the octahedral structure of MK was broken (Barbosa et al., 2018). The peaks at 640 cm^{-1} are associated with symmetric and asymmetric Si-O-T (T = Si or Al) vibrations of the geopolymer. At 445 cm^{-1} , peaks related to the vibration of Si-O-Si and also Al-O-Si are observed in all samples (Somna et al., 2011).

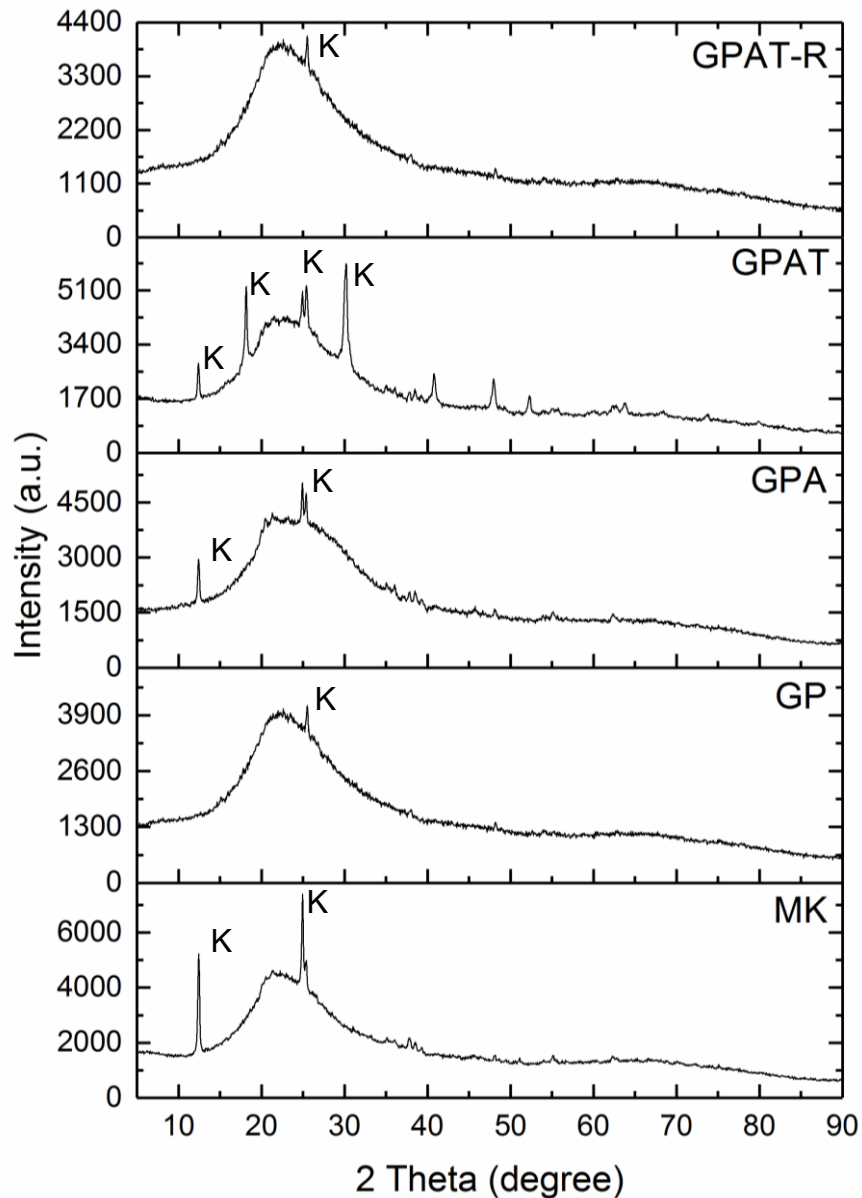
Fig. 16 - FTIR spectra of material and geopolymer modified.



Source: the author

The XRD spectra (Fig. 17) reveal that the MK and the formed geopolymers present an amorphous structure, with reflection between 15° and 30° (Simão et al., 2021). The predominant phase in metakaolin and geopolymers is quartz (K). It is observed at 25° that the quartz in the MK has high intensity, decreasing this peak with the formation of the GP, however, the treatment with acid and also with calcination, led again to the increase of the intensity of this crystalline phase.

Fig. 17 - XRD diffractograms of materials and modified geopolymer.

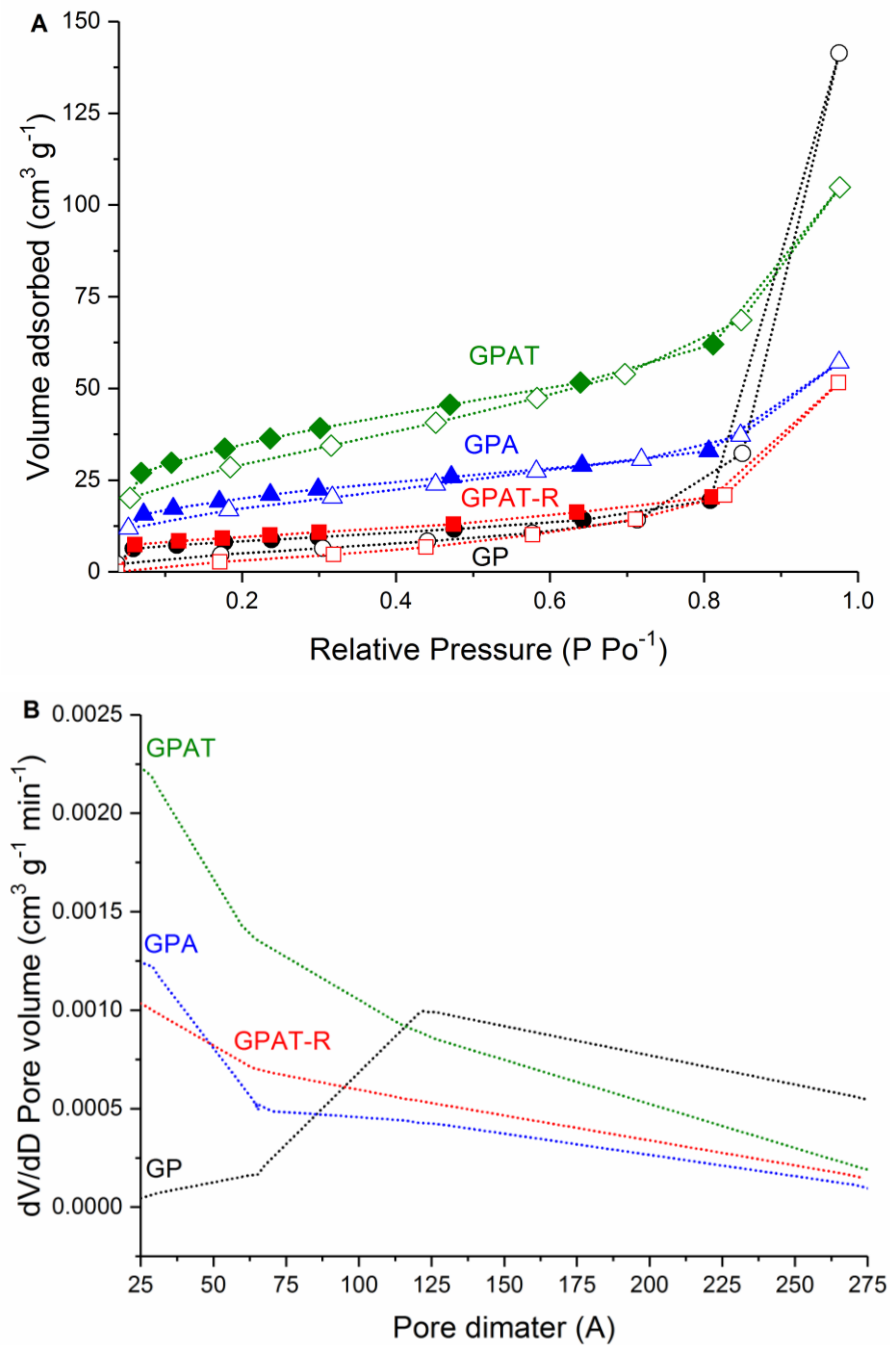


Note: MK – Metakaolin; GP – Geopolymer; GPA – Acid-modified geopolymer; GPAT – Geopolymer modified with acid and temperature; GPAT-A – Geopolymer modified with acid and temperature after adsorption; GPAT-R – Acid and temperature modified geopolymer regenerated.

Source: the author

Figure 18a shows the N₂ adsorption/desorption isotherm for GP modifications. The isotherms can be classified as type IV with small hysteresis, suggesting the presence of mesopores. The asymptotic vertical profile at high P/P₀ values is characteristic of meso and macroporous structures, with slit-shaped pores and non-uniform size (Thommes, 2010). In Figure 16b it is confirmed that the geopolymer and its modifications present a predominance of mesopores (2 nm ≤ pore size ≤ 50nm).

Fig. 18 – (a) Nitrogen adsorption/desorption isotherms and (b) pore size distribution of modified-GP.



Source: the author

The efficiency of an adsorbent is linked to the textural properties of the material, such as surface area, volume and pore diameter. In Table 15 these results are presented, and it is possible to observe an increase in the specific area with the treatments. The virgin GP presented a low area $S_{\text{BET}} = 29.67 \text{ m}^2 \text{ g}^{-1}$, with the acid attack, some tetrahedral structures of the material were broken, increasing the area to

70.48 m² g⁻¹. The thermal treatment, with calcination, helped to open new pores, increasing the area to 122 m² g⁻¹. The average pore volume and diameter in GP were larger than in GP-modified ones, as well as acid attack, several macro and mesopores gave rise to micropores that raised S_{BET}, while calcination promoted a doubling of the pore volume available for adsorption.

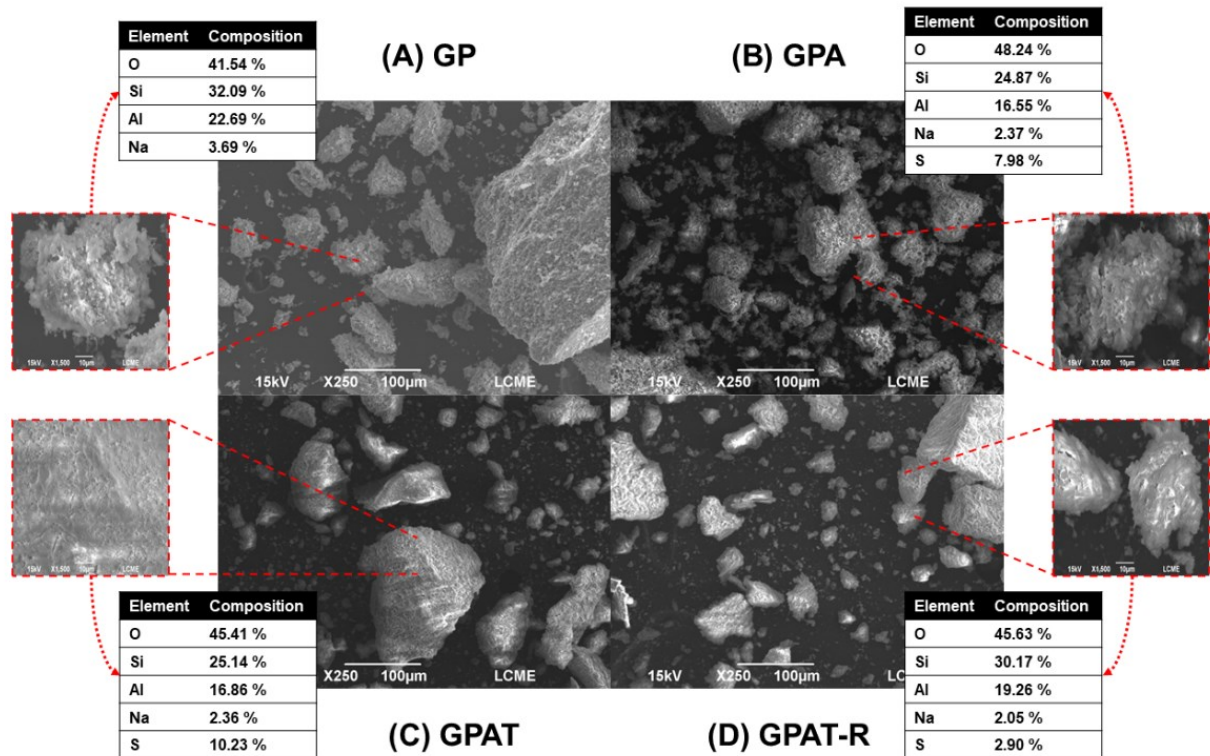
Table 15 - Textural properties of modified GPs

| Modified-GP | BET surface area (m ² g ⁻¹) | Pore volume (cm ³ g ⁻¹) | Mean pore diameter (nm) |
|-------------|---|---|-------------------------|
| GP | 29.67 | 0.223 | 5.358 |
| GPA | 70.48 | 0.062 | 2.145 |
| GPAT | 122.23 | 0.121 | 2.149 |
| GPAT-R* | 33.46 | 0.082 | 2.105 |

* Sample characterized after the 5th adsorption cycle

The SEM and EDS results for the GP and the modifications made are shown in Fig. 19. It is observed that the particles have a broad size range (roughly varying from 10 to 200 μm) with irregular shapes in all samples. The presence of silicon, aluminum, and sodium identified in the EDS was already expected from a geopolymerization reaction (De Rossi et al., 2020). Sulfur appears in GP samples modified with H₂SO₄. It is observed that the sulfur and sodium content decreases with GP regeneration, while the percentage of carbon increases.

Fig. 19 - SEM micrographs of (a) GP, (b) GPA, (c) GPAT, (d) GPAT-R and respective EDS analyses of the chemical elements identified.



Source: the author

3.4 FINAL CONSIDERATIONS

The modification was responsible for the increase in DR28 adsorption, obtaining removal percentages close to 100% and $q_e = 109 \text{ mg g}^{-1}$. The acid attack followed by calcination proved to be effective in increasing the surface area and the sites available for adsorption. The virgin GP area went from 29.67 to 122.23 $\text{m}^2 \text{g}^{-1}$ in GPAT. The investigated strategies for improving GP as a dye adsorbent were effective, with GPAT being a competitive adsorbent.

The adsorption equilibrium occurred in 150 min, however, for low concentrations (150 mg L^{-1}) in just 10 min, 95% of the dye was removed. The Elovich model had a good fit to the data, indicating that chemisorption has a strong influence. The isothermal tests indicated that the temperature has a positive effect, observing a significant increase in the adsorptive capacity ($20\text{-}110 \text{ mg g}^{-1}$), therefore, the Sips model was able to better represent the experimental data.

Although several azo compounds (acid, direct, reactive, and disperse dye) were tested for the study of adsorbent selectivity, only the direct azo dye (DR28) had an important removal from the colored effluent, almost 100% in a wide range of pH (3-9). Alternatively, the adsorbent is not selective for other dye classes, which may have functional groups other than the azo group.

Each of the tested dyes has different dyeing mechanisms, being used in different application methodologies (with a variation of pH, temperature, process time, as well as chemical auxiliaries) in different fabrics. These results, we can only state that the aluminosilicate-based adsorbent studied and modified by acid attack and calcination had an excellent performance for direct azo dyes, for the whole class of azo compounds an optimization is required.

CHAPTER IV

Chapter IV represents a closure of this research, presenting the general conclusions and seeking to respond to the objectives and hypotheses initially proposed. Although many results have been obtained and presented in the course of this work, the research does not end. Suggestions for future work include modifications in the GP to improve adsorption performance.

4 CONCLUSIONS AND OUTLOOK

4.1 CONCLUSIONS

The effect of acid etching was explored, proving to be significant in increasing the adsorption and removal capacity of the dye. Although calcination was not statistically significant, experimental results showed that it contributed to the improvement of adsorptive properties.

The characterization tests proved that the modifications did not cause significant changes in the composition of the material; however, there was an increase in the active sites for adsorption.

The operational conditions for adsorption were explored, allowing to obtain the transport and thermodynamic parameters of the process.

The recyclability of the adsorbent was investigated and proved to be attractive, mainly due to the increase in adsorptive properties and reuse after 3 cycles of regeneration.

Selectivity also showed satisfactory results, allowing the use of GPAT for DR28 adsorption in a wide range of pH.

Thus, it is concluded that this work was successful, confirming that acid attack followed by calcination are interesting strategies to make GP a more competitive adsorbent.

4.2 SUGGESTIONS FOR FUTURE WORK

Some strategies are suggested to continue this work:

- Using H_2O_2 in the GP formulation to increase the porosity of the material without modifications;

- Using acid as an aluminosilicate activating agent seeking to promote greater porosity;
- Studying GP curing at temperatures above 200 °C to increase the specific area;
- Using cylindrical molds with pins to create voids, forming monoliths;
- Evaluating the production of monoliths by 3D printing;
- Placing the GP monolith in contact with acid to study the creation of pores;
- Evaluating the performance of the adsorption of GP without treatment, comparing with the modified ones;

REFERENCES

- Acisli, O., Acar, I., Khataee, A., 2020. Preparation of a fly ash-based geopolymer for removal of a cationic dye: Isothermal, kinetic and thermodynamic studies. *J. Ind. Eng. Chem.* 83, 53–63. <https://doi.org/10.1016/j.jiec.2019.11.012>
- Açışlı, Ö., Acar, İ., Khataee, A., 2022. Preparation of a surface modified fly ash-based geopolymer for removal of an anionic dye: Parameters and adsorption mechanism. *Chemosphere* 295, 133870. <https://doi.org/10.1016/j.chemosphere.2022.133870>
- Akar, S.T., Koc, E., Sayin, F., Kara, I., Akar, T., 2021. Design and modeling of the decolorization characteristics of a regenerable and eco-friendly geopolymer: Batch and dynamic flow mode treatment aspects. *J. Environ. Manage.* 298, 113548. <https://doi.org/10.1016/j.jenvman.2021.113548>
- Al-Ghouti, M.A., Al-Kaabi, M.A., Ashfaq, M.Y., Da'na, D.A., 2019. Produced water characteristics, treatment and reuse: A review. *J. Water Process Eng.* 28, 222–239. <https://doi.org/10.1016/j.jwpe.2019.02.001>
- Alouani, M. El, Saufi, H., Moutaoukil, G., Alehyen, S., Nematollahi, B., Belmaghraoui, W., Taibi, M., 2021. Application of geopolymers for treatment of water contaminated with organic and inorganic pollutants: State-of-the-art review. *J. Environ. Chem. Eng.* 9, 105095. <https://doi.org/10.1016/j.jece.2021.105095>
- Bakharev, T., 2005. Resistance of geopolymer materials to acid attack. *Cem. Concr. Res.* 35, 658–670. <https://doi.org/10.1016/j.cemconres.2004.06.005>
- Barbosa, T.R., Foletto, E.L., Dotto, G.L., Jahn, S.L., 2018. Preparation of mesoporous geopolymer using metakaolin and rice husk ash as synthesis precursors and its use as potential adsorbent to remove organic dye from aqueous solutions. *Ceram. Int.* 44, 416–423. <https://doi.org/10.1016/j.ceramint.2017.09.193>
- Chen, H., Dong, S., Zhang, Y., He, P., 2022. Robust structure regulation of geopolymer as novel efficient amine support to prepare high-efficiency CO₂ capture solid sorbent. *Chem. Eng. J.* 427, 131577. <https://doi.org/10.1016/j.cej.2021.131577>

- Chen, H., Zhang, Y.J., He, P.Y., Liu, L.C., 2021. Synthesis, characterization, and selective CO₂ capture performance of a new type of activated carbon-geopolymer composite adsorbent. *J. Clean. Prod.* 325, 129271. <https://doi.org/10.1016/j.jclepro.2021.129271>
- Chen, W., Mo, J., Du, X., Zhang, Z., Zhang, W., 2019. Biomimetic dynamic membrane for aquatic dye removal. *Water Res.* 151, 243–251. <https://doi.org/10.1016/j.watres.2018.11.078>
- Crini, G., 2006. Non-conventional low-cost adsorbents for dye removal: A review. *Bioresour. Technol.* 97, 1061–1085. <https://doi.org/10.1016/j.biortech.2005.05.001>
- Davidovits, J., 2017. Geopolymers: Ceramic-like inorganic polymers. *J. Ceram. Sci. Technol.* 8, 335–350. <https://doi.org/10.4416/JCST2017-00038>
- Davidovits, J., 1991. Geopolymers: Inorganic polymeric new materials. *J. Therm. Anal.* 37, 1633–1656. <https://doi.org/10.1007/bf01912193>
- De Rossi, A., Simão, L., Ribeiro, M.J., Hotza, D., Moreira, R.F.P.M., 2020. Study of cure conditions effect on the properties of wood biomass fly ash geopolymers. *J. Mater. Res. Technol.* 9, 7518–7528. <https://doi.org/10.1016/j.jmrt.2020.05.047>
- De Rossi, A., Simão, L., Ribeiro, M.J., Novais, R.M., Labrincha, J.A., Hotza, D., Moreira, R.F.P.M., 2019. In-situ synthesis of zeolites by geopolymerization of biomass fly ash and metakaolin. *Mater. Lett.* 236, 644–648. <https://doi.org/10.1016/j.matlet.2018.11.016>
- Duxson, P., Fernández-Jiménez, A., Provis, J.L., Lukey, G.C., Palomo, A., Van Deventer, J.S.J., 2007. Geopolymer technology: The current state of the art. *J. Mater. Sci.* 42, 2917–2933. <https://doi.org/10.1007/s10853-006-0637-z>
- Duxson, P., Provis, J.L., Lukey, G.C., Mallicoat, S.W., Kriven, W.M., Van Deventer, J.S.J., 2005. Understanding the relationship between geopolymer composition, microstructure and mechanical properties. *Colloids Surfaces A Physicochem. Eng. Asp.* 269, 47–58. <https://doi.org/10.1016/j.colsurfa.2005.06.060>

- Feng, X., Yan, S., Jiang, S., Huang, K., Ren, X., Du, X., Xing, P., 2021. Green synthesis of the metakaolin/slag based geopolymer for the effective removal of methylene blue and Pb (II). *Silicon* 1, 1–15. <https://doi.org/10.1007/s12633-021-01439-z>
- Franchin, G., Pesonen, J., Luukkonen, T., Bai, C., Scanferla, P., Botti, R., Carturan, S., Innocentini, M., Colombo, P., 2020. Removal of ammonium from wastewater with geopolymer sorbents fabricated via additive manufacturing. *Mater. Des.* 195, 109006. <https://doi.org/10.1016/j.matdes.2020.109006>
- Fumba, G., Essomba, J.S., Merlain Tagne, G., Nsami, J.N., Désiré, P., Bélibi, B., Mbadcam, J.K., 2014. Equilibrium and kinetic adsorption studies of methyl orange from aqueous solutions using kaolinite, metakaolinite and activated geopolymer as low cost adsorbents. *J. Acad. Ind. Res.* 3, 156.
- Geng, J.J., Zhou, M., Li, Y., Chen, Y., Han, Y., Wan, S., Zhou, X., Hou, H., 2017. Comparison of red mud and coal gangue blended geopolymers synthesized through thermal activation and mechanical grinding preactivation. *Constr. Build. Mater.* 153, 185–192. <https://doi.org/10.1016/j.conbuildmat.2017.07.045>
- Guo, C.M., Wang, K.T., Liu, M.Y., Li, X.H., Cui, X.M., 2016. Preparation and characterization of acid-based geopolymer using metakaolin and disused polishing liquid. *Ceram. Int.* 42, 9287–9291. <https://doi.org/10.1016/j.ceramint.2016.02.073>
- Hosseini Asl, S.M., Javadian, H., Khavarpour, M., Belviso, C., Taghavi, M., Maghsudi, M., 2019. Porous adsorbents derived from coal fly ash as cost-effective and environmentally-friendly sources of aluminosilicate for sequestration of aqueous and gaseous pollutants: A review. *J. Clean. Prod.* 208, 1131–1147. <https://doi.org/10.1016/j.jclepro.2018.10.186>
- Hua, P., Sellaoui, L., Franco, D., Netto, M.S., Luiz Dotto, G., Bajahzar, A., Belmabrouk, H., Bonilla-Petriciolet, A., Li, Z., 2020. Adsorption of acid green and procion red on a magnetic geopolymer based adsorbent: Experiments, characterization and theoretical treatment. *Chem. Eng. J.* 383, 123113. <https://doi.org/10.1016/j.cej.2019.123113>

- Huang, Q., Liu, M., Mao, L., Xu, D., Zeng, G., Huang, H., Jiang, R., Deng, F., Zhang, X., Wei, Y., 2017. Surface functionalized SiO₂ nanoparticles with cationic polymers via the combination of mussel inspired chemistry and surface initiated atom transfer radical polymerization: Characterization and enhanced removal of organic dye. *J. Colloid Interface Sci.* 499, 170–179. <https://doi.org/10.1016/j.jcis.2017.03.102>
- Izquierdo, M., Querol, X., Phillipart, C., Antenucci, D., Towler, M., 2010. The role of open and closed curing conditions on the leaching properties of fly ash-slag-based geopolymers. *J. Hazard. Mater.* 176, 623–628. <https://doi.org/10.1016/j.jhazmat.2009.11.075>
- Ji, Z., Su, L., Pei, Y., 2021. Characterization and adsorption performance of waste-based porous open-cell geopolymer with one-pot preparation. *Ceram. Int.* 47, 12153–12162. <https://doi.org/10.1016/j.ceramint.2021.01.062>
- Jin, H., Zhang, Y., Wang, Q., Chang, Q., Li, C., 2021. Rapid removal of methylene blue and nickel ions and adsorption/desorption mechanism based on geopolymer adsorbent. *Colloid Interface Sci. Commun.* 45, 100551. <https://doi.org/10.1016/j.colcom.2021.100551>
- Khalid, H.R., Lee, N.K., Park, S.M., Abbas, N., Lee, H.K., 2018. Synthesis of geopolymer-supported zeolites via robust one-step method and their adsorption potential. *J. Hazard. Mater.* 353, 522–533. <https://doi.org/10.1016/j.jhazmat.2018.04.049>
- Khan, M.I., Azizli, K., Sufian, S., Man, Z., 2015a. Sodium silicate-free geopolymers as coating materials: Effects of Na/Al and water/solid ratios on adhesion strength. *Ceram. Int.* 41, 2794–2805. <https://doi.org/10.1016/j.ceramint.2014.10.099>
- Khan, M.I., Min, T.K., Azizli, K., Sufian, S., Ullah, H., Man, Z., 2015b. Effective removal of methylene blue from water using phosphoric acid based geopolymers: Synthesis, characterizations and adsorption studies. *RSC Adv.* 5, 61410–61420. <https://doi.org/10.1039/c5ra08255b>
- Komnitsas, K., Zaharaki, D., 2007. Geopolymerisation: A review and prospects for the minerals industry. *Miner. Eng.* 20, 1261–1277.

<https://doi.org/10.1016/j.mineng.2007.07.011>

- Lan, T., Li, P., Rehman, F.U., Li, X., Yang, W., Guo, S., 2019. Efficient adsorption of Cd²⁺ from aqueous solution using metakaolin geopolymers. *Environ. Sci. Pollut. Res.* 26, 33555–33567. <https://doi.org/10.1007/s11356-019-06362-w>
- Lee, N.K., Khalid, H.R., Lee, H.K., 2016. Synthesis of mesoporous geopolymers containing zeolite phases by a hydrothermal treatment. *Microporous Mesoporous Mater.* 229, 22–30. <https://doi.org/10.1016/j.micromeso.2016.04.016>
- Li, C.J., Zhang, Y.J., Chen, H., He, P.Y., Meng, Q., 2022. Development of porous and reusable geopolymer adsorbents for dye wastewater treatment. *J. Clean. Prod.* 348, 131278. <https://doi.org/10.1016/j.jclepro.2022.131278>
- Li, L., Wang, S., Zhu, Z., 2006. Geopolymeric adsorbents from fly ash for dye removal from aqueous solution. *J. Colloid Interface Sci.* 300, 52–59. <https://doi.org/10.1016/j.jcis.2006.03.062>
- Mo, J., Yang, Q., Zhang, N., Zhang, W., Zheng, Y., Zhang, Z., 2018. A review on agro-industrial waste (AIW) derived adsorbents for water and wastewater treatment. *J. Environ. Manage.* 227, 395–405. <https://doi.org/10.1016/j.jenvman.2018.08.069>
- Mohapatra, S.S., Mishra, J., Nanda, B., Patro, S.K., 2022. A review on waste-derived alkali activators for preparation of geopolymer composite. *Mater. Today Proc.* 56, 440–446. <https://doi.org/10.1016/j.matpr.2022.01.400>
- Netto, M.S., Rossatto, D.L., Jahn, S.L., Mallmann, E.S., Dotto, G.L., Foletto, E.L., 2020. Preparation of a novel magnetic geopolymer/zero-valent iron composite with remarkable adsorption performance towards aqueous Acid Red 97. *Chem. Eng. Commun.* 207, 1048–1061. <https://doi.org/10.1080/00986445.2019.1635467>
- Novais, R.M., Ascensão, G., Ferreira, N., Seabra, M.P., Labrincha, J.A., 2018a. Influence of water and aluminium powder content on the properties of waste-containing geopolymer foams. *Ceram. Int.* 44, 6242–6249. <https://doi.org/10.1016/j.ceramint.2018.01.009>

- Novais, R.M., Ascensão, G., Tobaldi, D.M., Seabra, M.P., Labrincha, J.A., 2018b. Biomass fly ash geopolymer monoliths for effective methylene blue removal from wastewaters. *J. Clean. Prod.* 171, 783–794. <https://doi.org/10.1016/j.jclepro.2017.10.078>
- Novais, R.M., Buruberri, L.H., Seabra, M.P., Labrincha, J.A., 2016. Novel porous fly-ash containing geopolymer monoliths for lead adsorption from wastewaters. *J. Hazard. Mater.* 318, 631–640. <https://doi.org/10.1016/j.jhazmat.2016.07.059>
- Novais, R.M., Carvalheiras, J., Tobaldi, D.M., Seabra, M.P., Pullar, R.C., Labrincha, J.A., 2019. Synthesis of porous biomass fly ash-based geopolymer spheres for efficient removal of methylene blue from wastewaters. *J. Clean. Prod.* 207, 350–362. <https://doi.org/10.1016/j.jclepro.2018.09.265>
- Novais, R.M., Pullar, R.C., Labrincha, J.A., 2020. Geopolymer foams: An overview of recent advancements. *Prog. Mater. Sci.* 109, 100621. <https://doi.org/10.1016/j.pmatsci.2019.100621>
- Oliveira, K.G., Botti, R., Kavun, V., Gafiullina, A., Franchin, G., Repo, E., Colombo, P., 2022. Geopolymer beads and 3D printed lattices containing activated carbon and hydrotalcite for anionic dye removal. *Catal. Today* 390–391, 57–68. <https://doi.org/10.1016/j.cattod.2021.12.002>
- Pan, B., Xing, B., 2008. Adsorption mechanisms of organic chemicals on carbon nanotubes. *Environ. Sci. Technol.* 42, 9005–9013. <https://doi.org/10.1021/es801777n>
- Pan, Y., Bai, Y., Chen, C., Yao, S., Tian, Q., Zhang, H., 2023. Effect of calcination temperature on geopolymer for the adsorption of cesium. *Mater. Lett.* 330, 133355. <https://doi.org/10.1016/j.matlet.2022.133355>
- Qiu, X., Liu, Y., Li, D., Yan, C., 2015. Preparation of NaP zeolite block from fly ash-based geopolymer via in situ hydrothermal method. *J. Porous Mater.* 22, 291–299. <https://doi.org/10.1007/s10934-014-9895-3>
- Ren, B., Zhao, Y., Bai, H., Kang, S., Zhang, T., Song, S., 2021. Eco-friendly geopolymer prepared from solid wastes: A critical review. *Chemosphere* 267,

128900. <https://doi.org/10.1016/j.chemosphere.2020.128900>

Rossatto, D.L., Netto, M.S., Jahn, S.L., Mallmann, E.S., Dotto, G.L., Foletto, E.L., 2020. Highly efficient adsorption performance of a novel magnetic geopolymer/Fe₃O₄ composite towards removal of aqueous acid green 16 dye. *J. Environ. Chem. Eng.* 8, 103804. <https://doi.org/10.1016/j.jece.2020.103804>

Ruthven, D.M., 1984. *Principles of Adsorption and Adsorption processes.*

Sanguanpak, S., Wannagon, A., Saengam, C., Chiemchaisri, W., Chiemchaisri, C., 2021. Porous metakaolin-based geopolymer granules for removal of ammonium in aqueous solution and anaerobically pretreated piggery wastewater. *J. Clean. Prod.* 297, 126643. <https://doi.org/10.1016/j.jclepro.2021.126643>

Selkälä, T., Suopajarvi, T., Sirviö, J.A., Luukkonen, T., Kinnunen, P., De Carvalho, A.L.C.B., Liimatainen, H., 2020. Surface modification of cured inorganic foams with cationic cellulose nanocrystals and their use as reactive filter media for anionic dye removal. *ACS Appl. Mater. Interfaces* 12, 27745–27757. <https://doi.org/10.1021/acsami.0c05927>

Simão, Lisandro, De Rossi, A., Hotza, D., Ribeiro, M.J., Novais, R.M., Klegues Montedo, O.R., Raupp-Pereira, F., 2021. Zeolites-containing geopolymers obtained from biomass fly ash: Influence of temperature, composition, and porosity. *J. Am. Ceram. Soc.* 104, 803–815. <https://doi.org/10.1111/jace.17512>

Simão, L., Fernandes, E., Hotza, D., Ribeiro, M.J., Montedo, O.R.K., Raupp-Pereira, F., 2021. Controlling efflorescence in geopolymers: A new approach. *Case Stud. Constr. Mater.* 15, e00740. <https://doi.org/10.1016/j.cscm.2021.e00740>

Simão, L., Hotza, D., Ribeiro, M.J., Novais, R.M., Montedo, O.R.K., Raupp-Pereira, F., 2020. Development of new geopolymers based on stone cutting waste. *Constr. Build. Mater.* 257, 119525. <https://doi.org/10.1016/j.conbuildmat.2020.119525>

Singh, N.B., Nagpal, G., Agrawal, S., Rachna, 2018. Water purification by using Adsorbents: A Review. *Environ. Technol. Innov.* 11, 187–240. <https://doi.org/10.1016/j.eti.2018.05.006>

- Sips, R., 1948. On the structure of a catalyst surface. *J. Chem. Phys.* 16, 490–495. <https://doi.org/10.1063/1.1746922>
- Siyal, A.A., Shamsuddin, M.R., Khan, M.I., Rabat, N.E., Zulfiqar, M., Man, Z., Siame, J., Azizli, K.A., 2018. A review on geopolymers as emerging materials for the adsorption of heavy metals and dyes. *J. Environ. Manage.* 224, 327–339. <https://doi.org/10.1016/j.jenvman.2018.07.046>
- Somna, K., Jaturapitakkul, C., Kajitvichyanukul, P., Chindaprasirt, P., 2011. NaOH-activated ground fly ash geopolymer cured at ambient temperature. *Fuel* 90, 2118–2124. <https://doi.org/10.1016/j.fuel.2011.01.018>
- Thommes, M., 2010. Physical adsorption characterization of nanoporous materials. *Chemie Ing. Tech.* 82, 1059–1073. <https://doi.org/10.1002/cite.201000064>
- Tian, Q., Wang, H., Pan, Y., Bai, Y., Chen, C., Yao, S., Guo, B., Zhang, H., 2022. Immobilization mechanism of cesium in geopolymer: Effects of alkaline activators and calcination temperature. *Environ. Res.* 215, 114333. <https://doi.org/10.1016/j.envres.2022.114333>
- Tochetto, Gabriel A., da Silva, T.C., Bampi, J., de F. P. M. Moreira, R., da Luz, C., Pasquali, G.D.L., Dervanoski, A., 2022. Conversion of *Syagrus romanzoffiana* into high-efficiency biosorbent for dye removal from synthetic and real textile effluent. *Water, Air, Soil Pollut.* 233, 252. <https://doi.org/10.1007/s11270-022-05737-z>
- Tochetto, G.A., Simão, L., de Oliveira, D., Hotza, D., Immich, A.P.S., 2022. Porous geopolymers as dye adsorbents: Review and perspectives. *J. Clean. Prod.* 374, 133982. <https://doi.org/10.1016/j.jclepro.2022.133982>
- Tome, S., Hermann, D.T., Shikuku, V.O., Otieno, S., 2021. Synthesis, characterization and application of acid and alkaline activated volcanic ash-based geopolymers for adsorptive remotion of cationic and anionic dyes from water. *Ceram. Int.* 47, 20965–20973. <https://doi.org/10.1016/j.ceramint.2021.04.097>
- Toniolo, N., Rincón, A., Roether, J.A., Ercole, P., Bernardo, E., Boccaccini, A.R., 2018. Extensive reuse of soda-lime waste glass in fly ash-based geopolymers. *Constr. Build. Mater.* 188, 1077–1084. <https://doi.org/10.1016/j.conbuildmat.2018.08.096>

- Trincal, V., Benavent, V., Lahalle, H., Balsamo, B., Samson, G., Patapy, C., Jainin, Y., Cyr, M., 2022. Effect of drying temperature on the properties of alkali-activated binders - Recommendations for sample preconditioning. *Cem. Concr. Res.* 151, 106617. <https://doi.org/10.1016/j.cemconres.2021.106617>
- van Eck, N.J., Waltman, L., 2010. Software survey: VOSviewer, a computer program for bibliometric mapping. *Scientometrics* 84, 523–538. <https://doi.org/10.1007/s11192-009-0146-3>
- Wang, J., Guo, X., 2020. Adsorption kinetic models: Physical meanings, applications, and solving methods. *J. Hazard. Mater.* 390, 122156. <https://doi.org/10.1016/j.jhazmat.2020.122156>
- Waring, D.R., Hallas, G., 1990. *The Chemistry and Application of Dyes*. Springer US, Boston, MA. <https://doi.org/10.1007/978-1-4684-7715-3>
- Xu, F., Gu, G., Zhang, W., Wang, H., Huang, X., Zhu, J., 2018. Pore structure analysis and properties evaluations of fly ash-based geopolymer foams by chemical foaming method. *Ceram. Int.* 44, 19989–19997. <https://doi.org/10.1016/j.ceramint.2018.07.267>
- Xu, H., Van Deventer, J.S.J., 2000. The geopolymerisation of alumino-silicate minerals. *Int. J. Miner. Process.* 59, 247–266. [https://doi.org/10.1016/S0301-7516\(99\)00074-5](https://doi.org/10.1016/S0301-7516(99)00074-5)
- Yagub, M.T., Sen, T.K., Afroze, S., Ang, H.M., 2014. Dye and its removal from aqueous solution by adsorption: A review. *Adv. Colloid Interface Sci.* 209, 172–184. <https://doi.org/10.1016/j.cis.2014.04.002>
- Zhang, M., Zhao, M., Zhang, G., Mann, D., Lumsden, K., Tao, M., 2016. Durability of red mud-fly ash based geopolymer and leaching behavior of heavy metals in sulfuric acid solutions and deionized water. *Constr. Build. Mater.* 124, 373–382. <https://doi.org/10.1016/j.conbuildmat.2016.07.108>
- Zhang, X., Bai, C., Qiao, Y., Wang, X., Jia, D., Li, H., Colombo, P., 2021. Porous geopolymer composites: A review. *Compos. Part A Appl. Sci. Manuf.* 150, 106629. <https://doi.org/10.1016/j.compositesa.2021.106629>

- Zhang, Xuhao, Zhang, Xiao, Li, X., Tian, D., Ma, M., Wang, T., 2022. Optimized pore structure and high permeability of metakaolin/fly-ash-based geopolymer foams from Al- and H₂O₂-sodium oleate foaming systems. *Ceram. Int.* 48, 18348–18360. <https://doi.org/10.1016/j.ceramint.2022.03.094>
- Zhang, Z., Li, L., He, D., Ma, X., Yan, C., Wang, H., 2016. Novel self-supporting zeolitic block with tunable porosity and crystallinity for water treatment. *Mater. Lett.* 178, 151–154. <https://doi.org/10.1016/j.matlet.2016.04.214>
- Zribi, M., Samet, B., Baklouti, S., 2019. Effect of curing temperature on the synthesis, structure and mechanical properties of phosphate-based geopolymers. *J. Non. Cryst. Solids* 511, 62–67. <https://doi.org/10.1016/j.jnoncrysol.2019.01.032>